https://doi.org/10.1093/plphys/kiad415 PLANT PHYSIOLOGY 2024: 194: 33–50

Plant Physiology®

Update

Enzymes in 3D: Synthesis, remodelling, and hydrolysis of cell wall (1,3;1,4)-β-glucans

Maria Hrmova,[1] Jochen Zimmer,[2] Vincent Bulone[3,4] and Geoffrey B. Fincher[1,*]

1 School of Agriculture, Food and Wine, and the Waite Research Institute, University of Adelaide, Glen Osmond, South Australia 5064, Australia
2 Howard Hughes Medical Institute and Department of Molecular Physiology and Biological Physics, University of Virginia School of Medicine, Charlottesville, VA 22908, USA
3 College of Medicine and Public Health, Flinders University, Bedford Park, South Australia 5042, Australia
4 Division of Glycoscience, Department of Chemistry, KTH Royal Institute of Technology, Alba Nova University Centre, 106 91 Stockholm, Sweden

*Author for correspondence: geoff.fincher@adelaide.edu.au
The author responsible for distribution of materials integral to the findings presented in this article in accordance with the policy described in the Instructions for Authors (https://academic.oup.com/plphys/pages/general-instructions) is: Geoff Fincher (geoff.fincher@adelaide.edu.au).

Abstract

Recent breakthroughs in structural biology have provided valuable new insights into enzymes involved in plant cell wall metabolism. More specifically, the molecular mechanism of synthesis of (1,3;1,4)-β-glucans, which are widespread in cell walls of commercially important cereals and grasses, has been the topic of debate and intense research activity for decades. However, an inability to purify these integral membrane enzymes or apply transgenic approaches without interpretative problems associated with pleiotropic effects has presented barriers to attempts to define their synthetic mechanisms. Following the demonstration that some members of the CslF sub-family of GT2 family enzymes mediate (1,3;1,4)-β-glucan synthesis, the expression of the corresponding genes in a heterologous system that is free of background complications has now been achieved. Biochemical analyses of the (1,3;1,4)-β-glucan synthesized in vitro, combined with 3-dimensional (3D) cryogenic-electron microscopy and AlphaFold protein structure predictions, have demonstrated how a single CslF6 enzyme, without exogenous primers, can incorporate both (1,3)- and (1,4)-β-linkages into the nascent polysaccharide chain. Similarly, 3D structures of xyloglucan endo-transglycosylases and (1,3;1,4)-β-glucan endo- and exohydrolases have allowed the mechanisms of (1,3;1,4)-β-glucan modification and degradation to be defined. X-ray crystallography and multi-scale modeling of a broad specificity GH3 β-glucan exohydrolase recently revealed a previously unknown and remarkable molecular mechanism with reactant trajectories through which a polysaccharide exohydrolase can act with a processive action pattern. The availability of high-quality protein 3D structural predictions should prove invaluable for defining structures, dynamics, and functions of other enzymes involved in plant cell wall metabolism in the immediate future.

Introduction

Structural biology has enabled some of humanity's most momentous discoveries. Crystal structures of proteins (Corey and Pauling 1953), DNA (Watson and Crick 1953; Bernal 1958), and RNA (Cate et al. 1996) have allowed us not only to describe the 3-dimensional (3D) structures at the atomic level, and hence the functions of these molecules, but have also allowed us to develop and describe key metabolic processes, including ribozyme function and CRISPR gene editing (Wang et al. 2022). However, structural biology technologies are experimentally difficult, and, as a result, their application in plant cell wall biology has been limited. Crystallizing soluble enzymes involved in wall metabolism has been achieved

Received May 18, 2023. Accepted June 09, 2023. Advance access publication August 18, 2023

Open Access

ADVANCES BOX

- 3D structures of participating enzymes provide new insights into the molecular mechanisms of both (1,3;1,4)-β-glucan synthesis and hydrolysis
- A single barley *CslF6* gene expressed in insect cells synthesizes (1,3;1,4)-β-glucans of DP up to 100 or more, without exogenous primers
- Structural biology has demonstrated how (1,3)- and (1,4)-β-linkages can be inserted into the elongating chain
- Evolutionary changes in the cellulose synthase gene super-family that allow this unique specificity have been identified
- X-ray crystallographic and multiscale molecular modeling analyses of the barley β-glucan exohydrolase *Exo*1 explain its broad specificity, its reactant trajectories, and a processive action pattern previously unrecognized in polysaccharide exohydrolase.

relatively rarely, and obtaining 3D data for the integral membrane enzymes that mediate the synthesis of many wall polysaccharides has proved to be particularly challenging. Although X-ray crystallography has been the key method in the past, the achievement of atomic resolution through cryogenic-electron microscopy (cryo-EM) has been a major breakthrough for studying membrane-integrated proteins and those attached to flexible polymers (Kühlbrandt 2014; Bartesaghi et al. 2015; Yip et al. 2020).

Here we review recent advances in our understanding of 3D structures of enzymes involved in the synthesis, remodeling, and hydrolysis of key cell wall polysaccharides. This knowledge advances our understanding of the molecular mechanisms of catalysis and the evolutionary dynamics of the corresponding genes involved in the synthesis of these polysaccharides. The review is focused on the structural biology of enzymes that mediate the metabolism of (1,3;1,4)-β-glucans, which are commonly found in walls of the Poaceae.

The unique structures of (1,3;1,4)-β-glucans

The (1,3;1,4)-β-glucans are widely distributed but not ubiquitous in cell walls of the grasses, where they constitute 0.5% to 2.3% of walls in wheat grains, 2% to 10% in walls of barley, and 3.8% to 6.1% of walls in oat grains (Fincher and Stone 2004). They have also been detected, but not quantitated, in other commelinid and noncommelinid species and nonmonocot taxa, including the monilophyte genus *Equisetum*, some bryophytes, certain green and red algae, lichens, a fungus, and a chromalveolate (Harris and Fincher 2009; Little et al. 2018).

In the water-soluble (1,3;1,4)-β-glucan from the starchy endosperm of barley, there are about 70% (1,4)-linkages and 30% (1,3)-linkages between glucosyl residues (Woodward et al. 1983). In general, single (1,3)-linkages are separated by groups of mainly 2 or three adjacent (1,4)-linkages, but with approximately 10% of the polysaccharide comprising blocks of up to 10 or more adjacent (1,4)-linkages (Woodward et al. 1983). More than 1 adjacent (1,3)-linkage is rarely if ever found (Woodward et al. 1983; Buliga et al. 1986). When the polysaccharide is hydrolyzed with specific (1,3;1,4)-β-glucan endohydrolases, which only hydrolyze (1,4)-linkages on the reducing terminal side of a (1,3)-linked β-glucosyl residue, the trisaccharide $G4G3G_{red}$ (DP3) and tetrasaccharide $G4G4G3G_{red}$ (DP4) are the major products (where G represents a glucosyl residue, 3 and 4 are the β-linkage types, $_{red}$ denotes the reducing end of the oligosaccharide, and DP is degree of polymerization) (Woodward et al. 1983). Markov chain analyses of the oligosaccharides in partial hydrolysates of the polysaccharide showed that these tri- and tetrasaccharides are arranged randomly along the backbone chain (Staudte et al. 1983). Thus, the polysaccharide structure has a random component with respect to the arrangement of the tri- and tetrasaccharides but a nonrandom component insofar as only single (1,3)-linkages are present. Given that approximately 30% of the polymer consists of (1,3)-linked glucosyl residues, if these (1,3)-linkages were arranged randomly, one would expect to find multiple regions of 2 or more adjacent (1,3)-linkages. The distribution patterns of the longer blocks of adjacent (1,4)-linkages have not been defined.

While a few other polysaccharides contain different linkage types in the main chain, such as the bacterial SIII pneumococcal polysaccharide that is composed of a repeating sequence of (1,3)-β-linked cellobiuronic acid residues (Anderson and Stone 1975) and hyaluronan, which is composed of a repeating disaccharide of N-acetylglucosaminosyl and glucuronosyl acid residues that has alternating (1,3)-β- and (1,4)-β-linkages (Weigel and DeAngelis 2007; Maloney et al. 2022), both of these polysaccharides are characterized by strictly repeating disaccharide moieties.

Superimposed on these structural complexities of (1,3;1,4)-β-glucans is the high degree of variability in their fine structure. The proportions of (1,3)- and (1,4)-linkages can vary from species to species and within walls of different tissues in a single species, and, as a result, the relative proportions of the DP3 and DP4 oligosaccharides will also vary. Lazaridou and Biliaderis (2007) used DP3:DP4 ratios to distinguish between (1,3;1,4)-β-glucans from different sources and noted the link between the ratios and polysaccharide solubility. As a result of different spatial and bonding interactions between adjacent glucosyl residues, (1,3)-β-glucosyl linkages are inherently more flexible than (1,4)-β-glucosyl linkages and form a molecular kink between the "cellulosic" oligosaccharides in the (1,3;1,4)-β-glucan backbone chain. Regular spacing of (1,3)-linkages would enable the polysaccharides to align in solution, and their solubility would thereby be reduced. The random arrangement of the DP3 and DP4 units indicates that the (1,3)-linkages are not evenly spaced along

the chain and is responsible, at least in part, for the relative solubility of the polysaccharide in water. One can also conclude that the further the DP3:DP4 ratio deviates from 1.0 in either direction, the less soluble the polysaccharide is in aqueous solution (Burton et al. 2010). As an example of the differences in DP3:DP4 ratios between species, the storage (1,3;1,4)-β-glucan in the starchy endosperm of *Brachypodium distachyon* has a ratio of about 7:1 (Guillon et al. 2012), whereas the (1,3;1,4)-β-glucan from barley grain has a ratio of about 3:1 (Trafford et al. 2013).

Given this level of structural complexity and variability, it is perhaps not surprising that the molecular mechanism of (1,3;1,4)-β-glucan synthesis has intrigued biochemists for more than 50 years (e.g. Smith and Stone 1973), but progress toward understanding these mechanisms has been slow. More specifically, biochemists have addressed questions such as whether the (1,3)- and (1,4)-β-linkages are inserted into the nascent polysaccharide by a single enzyme or by multiple enzymes, how the random and nonrandom arrangements of linkage types are achieved, and whether oligosaccharide or other primers are required for the initiation of chain elongation. Our inability to purify these integral membrane enzymes has frustrated attempts to unequivocally answer these questions. The first significant advances were therefore achieved through the identification of the genes involved in (1,3;1,4)-β-glucan synthesis.

Discovery and characterization of genes encoding (1,3;1,4)-β-glucan synthases

Using comparative genomics based on quantitative trait loci and EST mapping, Burton et al. (2006) showed that certain members of the *CslF* gene subfamily of barley encoded (1,3;1,4)-β-glucan synthases. The *CslF* subfamily is classified within the GT2 family of processive glycosyl transferases, which contains a total of close to 50 *cellulose synthase* (*CesA*) genes and *cellulose synthase-like* (*Csl*) genes that mediate cell wall polysaccharide biosynthesis in angiosperms (Carbohydrate-Active enZymes database; http://www.cazy.org/; Drula et al. 2022). The *CslF* subfamily is monophyletic with the *CslD* subfamily, and it is likely that the *CslF* subfamily evolved relatively recently after the duplication of the *CslD*/*CslF* ancestor, which itself was derived from the *CesA* subfamily (Yin et al. 2014; Schwerdt et al. 2015; Dimitroff et al. 2016; Little et al. 2018). Thus, the closest relatives of the *CslF* genes are found in the *CslD* subfamily, which has been implicated in the synthesis of single (1,4)-β-glucan (cellulose) chains (Doblin et al. 2001; Bernal et al. 2008; Park et al. 2011; Yang et al. 2020).

Subsequent transcript profiling in the developing endosperm of barley indicated that *CslF6* transcripts were the most abundant, although there was a substantial peak of *CslF9* transcription early in grain development (Burton et al. 2008). The role of the CslF6 enzyme in (1,3;1,4)-β-glucan synthesis in cereal grains has been confirmed several times using various experimental approaches (Nemeth et al. 2010; Burton et al. 2011; Taketa et al. 2011; Vega-Sánchez et al. 2012), but there remains some doubt as to whether the CslF9 protein is directly involved in (1,3;1,4)-β-glucan synthesis (Garcia-Gimenez et al. 2020). For these reasons, the CslF6 enzyme has become the prime target in attempts to define the molecular mechanism of (1,3;1,4)-β-glucan synthesis. Advances in our understanding of this mechanism were provided through in vitro functional and structural analyses of the CslF6 enzyme (Purushotham et al. 2022).

The 3D structure of the CslF6 (1,3;1,4)-β-glucan synthase

Defining the 3D structures of integral membrane enzymes has proven to be particularly challenging. These membrane-spanning enzymes generally lose both their native 3D structure and activity when dissociated from the supporting membrane. A major advance in the field came when Morgan et al. (2013) published the 3D crystal structure of a catalytically active BcsA–BcsB complex of a cellulose synthase from the bacterium *Rhodobacter sphaeroides*, which shares sequence similarities with higher plant CesA enzymes. The BcsA component of the complex contains 8 transmembrane (TM) helices that surround a cylindrical channel through which the nascent cellulosic chain is extruded (Morgan et al. 2016).

The 3D structure of the bacterial BcsA protein agreed well with an ab initio predicted model for the catalytic domain of a cotton CesA enzyme (Sethaphong et al. 2013). The experimental and predicted structures confirmed the presence of spatially conserved active site D, D, TED, and QxxRW residues that represent invariant motifs across cellulose synthases and closely related enzymes (Richmond and Somerville 2000; Morgan et al. 2013). It also showed that plant-conserved regions and class-specific regions (CSR) (Fig. 1A) are located at the edge of the catalytic domain and that these 2 regions could be important in the CesA oligomerization that occurs in plant cellulose synthase complexes (Scavuzzo-Duggan et al. 2018; Purushotham et al. 2020). The GT2 family members are inverting enzymes that adopt an S_N2-like substitution reaction in which the OH group of the nascent polysaccharide's nonreducing terminal glycosyl residue acts as the nucleophilic acceptor and catalyzes an attack on the C1 carbon of the sugar nucleotide substrate's donor glycosyl residue; a base catalyst deprotonates the acceptor during the nucleophilic attack (Lairson et al. 2008; Fig. 1A).

The structures and models of the bacterial and cotton enzymes subsequently allowed homology modeling of the barley and sorghum CslF6 enzymes; these enzymes were chosen because of differences in the DP3:DP4 ratios of their (1,3;1,4)-β-glucans (Dimitroff et al. 2016). Heterologous expression of the 2 genes and various mutant variants in *Nicotiana benthamiana* identified several amino acid residues that affected the amount of (1,3;1,4)-β-glucan synthesized and the DP3:DP4 ratios. However, the data were

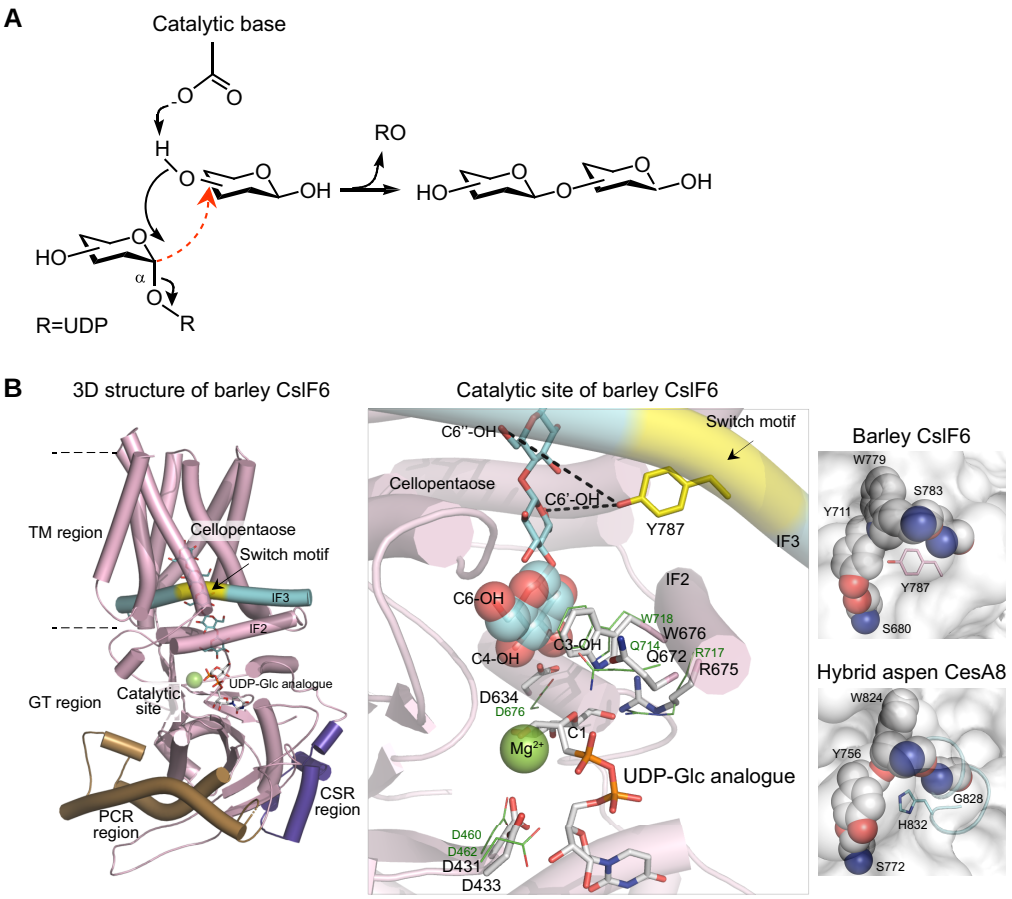

Figure 1. Catalytic mechanisms and 3D structures of the barley CslF6 (1,3:1,4)-β-glucan synthase and the hybrid aspen CesA8 cellulose synthase. **A)** Catalytic mechanism of GT2 enzymes where the catalytic base mediates transfer of a monosaccharide species from the nucleotide-sugar donor to acceptors, with the inversion of anomeric stereochemistry through an S_N2-like substitution reaction. The red arrow indicates where the new glycosidic linkage is formed. **B)** Left panel: Cartoon representation of the barley CslF6 enzyme (Purushotham et al. 2022). The structure is overlaid with cellopentaose-containing (cyan sticks) to illustrate the cellulose secretion path. The section of the IF3 helix representing the MTASCSAY switch is shown in yellow. The plant-conserved region α-helices (brown) and CSR (purple) regions are also specified. Middle panel: Position of conserved active site residues of CslF6 with D431 and D433 of the DxD motif, D634 (of the TED motif, catalytic base), Q672, R675, and W676 of the QxxRW, and Y787 residues of the switch motif (cpk sticks). The C6-OH groups of the acceptor substrate (cpk cyan sticks), the C3-OH and C4-OH groups of the terminal glucoside moiety (cpk cyan sticks and space fill representations), and the C1 atom of the UDP-Glc analogue in BcsA (PDB accession 5eiy) (cpk sticks) are labelled. Proposed interactions between the C6-OH group of the second and third Glc moieties (cyan) and the hydroxyl group of Y787 (cpk yellow sticks) are indicated in black dashes. Interface 2 (IF2) and IF3 α-helices (cyan) delineate the cytoplasmic boundary. The corresponding D462, D464, D676, Q714, R717, and W718 residues (green cpk lines) of CesA8 catalytic machinery are indicated (CslF6 and CesA8 superpose with an root-mean-square-deviation value of 1.76 Å). Right panels: Nearest interactions of the MTASCSAYL switch motif in barley CslF6, and of the corresponding VIGGVSAHL motif in CesA8 (Purushotham et al. 2020), with 4 residues (cpk spheres) surrounding Y787 (stick cpk magenta in CslF6; top) and H832 (stick cpk cyan in CesA8; bottom).

interpreted carefully because they were based on a molecular model and on heterologous expression in a plant system, where pleiotropic effects might distort protein folding (Jobling 2015; Dimitroff et al. 2016).

To overcome these limitations, a medium-resolution structure of the barley CslF6 enzyme was determined at an intermediate state during (1,3; 1,4)-β-glucan biosynthesis (Purushotham et al. 2022; Protein Data Bank [PDB] accession 8dqk) using cryo-EM coupled with AlphaFold protein structure predictions (Jumper et al. 2021) (Fig. 1B). The *CslF6* enzyme and several mutant forms were expressed in Sf9 insect cells, which were expected to have a "cleaner," nonplant background, and polysaccharides synthesized in vitro were analyzed (Purushotham et al. 2022).

Structural characteristics of the CslF6 (1,3;1,4)-β-glucan synthase

Several important enzymic characteristics were revealed in this study (Purushotham et al. 2022). Firstly, it was confirmed that the CslF6 enzyme adopts a CesA-like conformation, in which 7 transmembrane α-helices form a TM tunnel through which the nascent (1,3;1,4)-β-glucan is extruded across the membrane from the active site (Fig. 1B, left and middle

panels). Secondly, it was demonstrated that a single barley CslF6 enzyme was sufficient to synthesize a (1,3;1,4)-β-glucan with the same chemical properties as the (1,3;1,4)-β-glucan extracted from barley starchy endosperm. While it has been proposed that additional enzymes, such as (1,3)-β-glucan synthases or xyloglucan endo-transglycosylases (XETs) might be required for the insertion of the (1,3)-linkages into the elongating chain (Burton and Fincher 2009), Buckeridge et al. (2001) had correctly predicted that only 1 enzyme was necessary for the synthesis of (1,3;1,4)-β-glucans. It is important to note that during the expression of *CslF6* and its variants in Sf9 cells, polysaccharide chains of DP 25 to more than DP 100 were synthesized within 3 hours (Purushotham et al. 2022), without added primers. It is likely that the CslF6 enzyme initially hydrolyzes UDP-Glc and that the released glucose (Glc) acts as a self-priming acceptor for the initiation of (1,3;1,4)-β-glucan chain elongation, as demonstrated for hyaluronan and chitin synthases (Orlean and Funai 2019; Maloney et al. 2022). Thirdly, Purushotham et al. (2022) concluded that the CslF6 enzyme acted as a monomer in contrast to the trimeric and other oligomeric structures that form in higher plant CesA complexes (Purushotham et al. 2016, 2020; Jarvis 2018). Although CslF6 can be computationally assembled into similar homotrimeric complex, as observed for CesA, it is currently unclear why these complexes are not observed in vitro (Purushotham et al. 2022).

The CslF6 enzymes can be distinguished from other members of the CslF subfamily by the presence of a 40- to 50-amino acid residue insertion (Burton et al. 2008); the predicted length of this sequence varies according to the alignment programs used. Its approximate position on the lateral surface of the catalytic domain is indicated in Fig. 1B, but it appears to be flexible and unstructured and is part of the CSR of the enzyme. It is particularly rich in positively and negatively charged amino acid residues and might be involved in interactions with other proteins or phospholipids. Detailed knowledge of the 3D structure of the CslF6 enzyme subsequently allowed the definition of the enzyme's catalytic mechanism, through which both (1,3)- and (1,4)-linked glucosyl residues are incorporated into the elongating (1,3;1,4)-β-glucan chain.

Catalytic mechanism of the CslF6 (1,3;1,4)-β-glucan synthase

The 3D structure of the CslF6 enzyme revealed that its catalytic pocket is almost identical to the active site of the hybrid aspen CesA8 enzyme (PDB accession 6wlb) (Fig. 1B, middle panel; Purushotham et al. 2022). More specifically, strictly conserved residues implicated in binding the UDP-Glc substrate and coordinating the associated Mg^{2+} cation are positioned as observed in the CesA8 catalytic pocket (Fig. 1B, middle panel). The inevitable conclusion is that the UDP-Glc substrate is bound in the same position in both enzymes, relative to the acceptor. It follows that the positioning of the acceptor must account for the formation of (1,3)- and (1,4)-β-linkages by CslF6. Specifically, in the CesA8 enzyme, the C4-OH acceptor group on the nonreducing terminal of the nascent cellulosic chain is always in the same position relative to the catalytic base. However, in the CslF6 enzyme, the nonreducing terminal glucosyl residue of the polysaccharide chain acceptor is likely to be sufficiently mobile to allow the presentation of either the C3-OH or the C4-OH to the catalytic base and the C1 atom of the bound UDP-Glc.

In the case of the CesA8 enzyme, consecutive glucosyl residues of the nascent cellulosic chain are inverted by about 180° relative to each other so that the position of consecutive C4-OH groups in the active site is approximately the same relative to the substrate. Further, the nascent cellulose polymer translocates into the TM channel through a tube-like pore that constrains its movement, in particular at its terminal C4-OH. In contrast, (1,3)-β-glucans form a helical structure (Gidley and Nishinari 2009), and the 180° inversion observed between adjacent (1,4)-linked glucosyl residues does not occur between adjacent (1,3)- and (1,4)-linked residues. Thus, and as stated above, the 3D disposition of the elongating (1,3;1,4)-β-glucan chain's nonreducing end acceptor would need to be flexible enough to allow the addition of the incoming glucosyl residue to either the C3-OH or the C4-OH, which will be approximately 2 Å apart. The increased space required for this flexibility during (1,3;1,4)-β-glucan synthesis would likely involve relaxation of the putative CesA acceptor binding constraints and at the same time might allow an increase in the diameter of the pore leading from the active site into the TM channel.

Purushotham et al. (2022) therefore compared sequences of CesA, CslD, and CslF6 enzymes in this pore region and found that a conserved VIGGVSAHLF sequence in CesA enzymes (including the hybrid aspen CesA8 enzyme) and CslD enzymes was replaced by an MTASCSAYLA sequence in the CslF6 enzyme (Fig. 1B, left and middle panels). The CslF6 sequence was denoted the "switch" motif because of its probable role in the switch of substrate specificities between the 2 enzymes. The motif is highly conserved in CslF6 genes from other species (Purushotham et al. 2022), but it is not well conserved in other barley CslF enzymes. Nevertheless, the Y787 residue is always present. The H787Y mutation underlined in the motifs above appeared to be crucial for the formation of (1,3)-linkages by the CslF6 enzyme. Replacement of Y787 in CslF6 with a His residue (as found in the CesA sequence at that position; Fig. 1B, right panel) substantially reduced the number of (1,3)-linkages in the resultant polysaccharide; similar results were obtained if the entire switch motif of the CslF6 enzymes were replaced with the CesA8 motif. However, the reciprocal introduction of Y787 or the entire CslF6 motif into the CesA8 enzyme did not result in the formation of (1,3)-linkages (Purushotham et al. 2022). This suggests that while the switch motif is essential for (1,3)-linkage formation, additional structural adaptations

occurred during the evolution of CslF6 specificity, perhaps within the TM channel.

Despite these uncertainties, Purushotham et al. (2022) were able to propose a model for (1,3;1,4)-β-glucan synthesis in which it is assumed that CslF6 positions the accepting glucosyl unit similarly to that of CesA8 to favor glucosyl transfer to its C4-OH. However, interactions of the C6-OH of the second or third glucosyl residue from the nonreducing terminus of the elongating polysaccharide chain with switch motif's Y787 are proposed to reposition the acceptor to favor transfer to its C3-OH instead of the C4-OH. The precise mechanisms for controlling the insertion of single (1,3)-linkages, overall DP3:DP4 ratios, and the insertion of the longer blocks of adjacent (1,4)-linkages remain to be defined. In the latter case, the frequency of these longer blocks decreases with their DP (Woodward et al. 1983). Thus, as the length of adjacent (1,4)-linkages increases during synthesis, the chance of a (1,3)-linkage insertion increases. A higher-resolution 3D structure of the CslF6 enzyme and mutant variants, in complex with various donor and acceptor molecules, will enable these outstanding questions to be addressed.

Subcellular location of (1,3;1,4)-β-glucan synthesis

There are apparently conflicting data as to the subcellular site of (1,3; 1,4)-β-glucan synthesis. In angiosperms, it is generally accepted that noncellulosic wall polysaccharides are synthesized in the Golgi and subsequently transported to the plasma membrane and deposited in the wall (Carpita and McCann 2010; Dhugga 2012; Pauly et al. 2013). Carpita and McCann (2010) detected (1,3;1,4)-β-glucan in both cell walls and the Golgi in maize coleoptiles, and CslF proteins have been detected in highly enriched Golgi membranes from maize (Okekeogbu et al. 2019). Furthermore, live cell imaging and immuno-electron microscopy studies using a tagged CslF6 protein fusion from *B. distachyon* showed that, in yeast and tobacco heterologous expression systems, the enzyme was located in the Golgi apparatus, where (1,3;1,4)-β-glucan synthesis was also observed (Kim et al. 2015).

However, during a series of in situ immunocytochemical studies on cell cultures, developing endosperm and coleoptiles from barley, where (1,3;1,4)-β-glucan was abundant in cell walls, no (1,3;1,4)-β-glucan could be detected in the Golgi. This suggested that (1,3;1,4)-β-glucan synthesis was occurring at the plasma membrane in these tissues (Wilson et al. 2015), and it might be argued that the evolution of the CslF enzymes from CslD and CesA cellulose synthases (Yin et al. 2014; Schwerdt et al. 2015) would be consistent with this suggestion. However, there remain uncertainties associated with the interpretation of heterologous expression experiments, the difficulties experienced with the isolation of completely pure subcellular membrane preparations, the possibility that plasma membrane enzymes might be activated by cell disruption, and the question as to whether enzymes en route to the plasma membrane might also be active in the Golgi (Wightman and Turner 2008; Okekeogbu et al. 2019). Bulone et al. (2023) raised the possibility that (1,3;1,4)-β-glucans might be synthesized at either the plasma membrane or the Golgi, depending on the species, the tissue, the particular (1,3;1,4)-β-glucan synthase isoenzyme involved, and the developmental stage of the cell. In situ methods will be essential in future investigations of these variables. Emerging confocal, super-high resolution, and atomic force microscopy technologies (van de Meene et al. 2021) will undoubtedly allow these questions to be addressed.

Remodeling of (1,3;1,4)-β-glucans: Are xyloglucan endotransglycosylases (XETs) involved?

Despite the fact that cell walls in the Poaceae usually contain little or no xyloglucan, up to 40 *XET* and related xyloglucan hydrolase (*XEH*) genes of the GH16 family of glycoside hydrolases (Drula et al. 2022) are found in the barley genome (Stratilová et al. 2020; Akdemir et al. 2022), and high levels of *XET* transcripts are detected in tissues where wall components are being synthesized. These observations raise questions as to the biological role of the encoded enzymes in grass species (Burton and Fincher 2009). Hrmova et al. (2007) showed that a highly purified barley XET5 isoenzyme catalyzed the formation of covalent linkages between xyloglucans and either (1,3;1,4)-β-glucans or cellulosic polysaccharides in vitro. Hetero-transglycosylation reactions involving a (1,3;1,4)-β-glucan donor and various acceptors have also been observed in XETs from Arabidopsis, wheat, and *B. distachyon* XETs (Seven et al. 2021). Barley XET5 (Fig. 2A) has been allocated to the GH16_20 subfamily (Eklöf and Brumer 2010; Viborg et al. 2019), while a *Vitis vinifera* endoglucanase, which hydrolyzes both xyloglucan and (1,3;1,4)-β-glucan, represents a "specificity" intermediate between plant XTHs and bacterial lichenases of the GH16_21 subfamily; these intermediate forms are commonly found in the Poales (McGregor et al. 2017; Behar et al. 2018; Stratilová et al. 2020; Akdemir et al. 2022).

The obvious question then became whether the hetero-transglycosylation reactions catalyzed by the barley XET5 enzyme actually occurred in vivo or could simply be mechanistic when reactants were forced together in the in vitro assays. Stratilová et al. (2020) subsequently infiltrated young barley apical root segments with fluorescently labelled oligosaccharide probes to demonstrate that the barley XET enzymes were capable of in vivo hetero-transglycosylation involving a number of donor and acceptor molecules (Fig. 2B).

The crystal structure of a hybrid aspen XET has also been solved (PDB accession 1 μmz and 1 un1; Johansson et al. 2004). Here we used the AlphaFold protein structure model of the barley XET4 isoenzyme and docked the xyloglucan

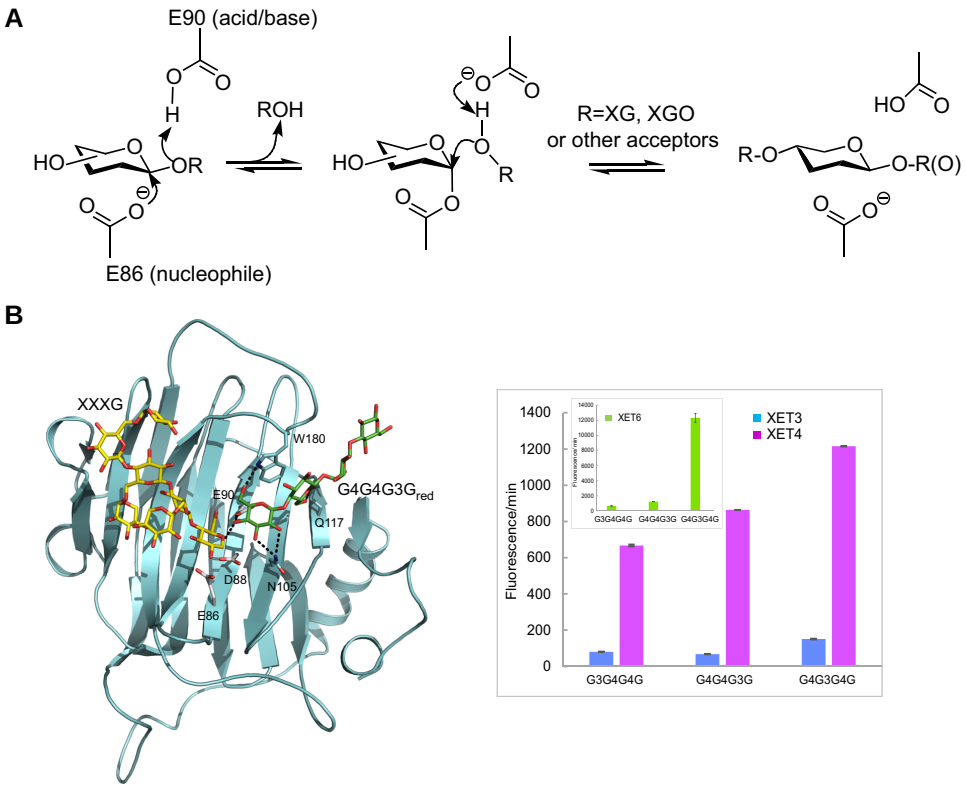

Figure 2. The catalytic mechanism and the 3D model of barley xyloglucan endotransglycosylase, isoenzyme XET4. **A)** Top panel: Catalytic mechanism of GH16 xyloglucan endotransglycosylases. The barley XET4 isoenzyme, with the assistance of E86 (nucleophile) and E90 (acid/base), mediates the transfer of saccharide substrates onto saccharide acceptors with the retention of stereochemistry through a double-displacement reaction (Johansson et al. 2004). **B)** Left panel: 3D model of barley XET4 isoenzyme (cyan) in complex with the docked XXXG hepta-saccharide donor (yellow cpk sticks)/tetra-saccharide G4G4G3G$_{red}$ acceptor (cpk sticks) substrate pair. Residues (cpk sticks) are within 2.6 to 3.4 Å separations (dashed lines) from the G4G4G3G$_{red}$ acceptor. Right panel: Hetero-transglycosylation reaction is catalyzed by barley XET3, XET4, and XET6 isoenzymes with xyloglucan donor/(1,3;1,4)-β-D-glucan acceptor/substrate and other pairs (Hrmova et al. 2009; Stratilová et al. 2020).

hepta-saccharide (XXXG) donor/tetra-saccharide G4G4G3G acceptor/substrate pair in the active site. Although the barley XET4 and XET5 enzymes belong to separate evolutionary lineages, both are able to use (1,3;1,4)-β-oligoglucosides as substrates (Hrmova et al. 2007; Stratilová et al. 2020). This simulation showed that the docked XXXG/G4G4G3G substrate pair can be favorably accommodated in the active site of barley XET4 isoenzyme (Fig. 2B), which explained why the barley XET4 catalyzes this hetero-transglycosylation reaction (Stratilová et al. 2020). It should be noted that we still do not know the biological significance or extent of these reactions involving (1,3;1,4)-β-glucan synthesis or remodeling during normal plant growth and development, which represents the next experimental target.

Hydrolysis of (1,3;1,4)-β-glucans: 3D folds, evolution, and enzymic mechanisms of β-glucan endohydrolases

The solubility and relatively small molecular sizes of many β-glucan endohydrolases have made them an easier target for X-ray crystallographic analyses than the membrane-bound β-glucan synthases. Varghese et al. (1994) solved the 3D structures of a barley (1,3)-β-glucan endohydrolase (isoenzyme GII) (PDB accession 1ghs) and a barley (1,3;1,4)-β-glucan endohydrolase (isoenzyme EII) (PDB accession 1ghr) to 2.2 Å and 2.3 Å resolution, respectively. The (1,3)-β-glucan endohydrolase hydrolyzes internal (1,3)-β-glucosyl linkages in (1,3)-β-glucans but has no action on (1,3;1,4)-β-glucans, which lack the adjacent (1,3)-β-glucosyl linkages necessary for hydrolysis by this enzyme. Conversely, the (1,3;1,4)-β-glucan endohydrolase only hydrolyzes (1,4)-linkages that are located toward the polysaccharide's reducing terminus of a (1,3)-linkage, as described above under (1,3;1,4)-β-glucan structure. The (1,3;1,4)-β-glucan endohydrolase has no activity on (1,3)-β-glucans or on (1,4)-β-glucans (Woodward et al. 1983).

Both enzymes are classified in the GH17 family of glycoside hydrolases (Drula et al. 2022), which use an acidic proton donor and a nucleophile/base to catalyze hydrolysis of the glycosidic linkage, using a double displacement mechanism with retention of anomeric configuration (Sinnott 1990; Namchuk and Withers 1995; Lairson et al. 2008; Fig. 3A).

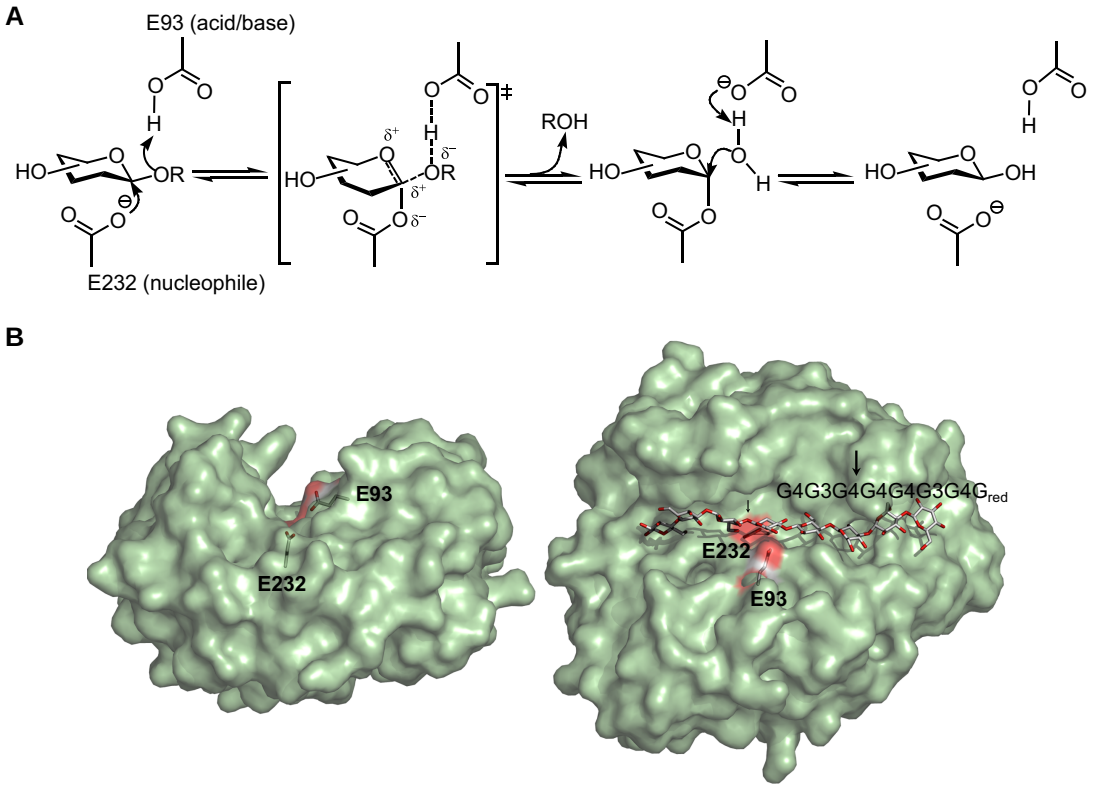

Figure 3. Catalytic mechanism and the crystal structure of the barley (1;3,1;4)-β-D-glucanase, isoenzyme EII. **A)** The barley GH17 (1;3,1;4)-β-D-glucanase EII, with the assistance of E232 (nucleophile) and E93 (acid/base) (Chen et al. 1993; Henrissat et al. 1995; Jenkins et al. 1995), catalyzes the hydrolysis of substrates with the retention of stereochemistry through a double-displacement reaction (Lairson et al. 2008). **B)** Molecular surface morphology of the (1;3,1;4)-β-D-glucanase, isoenzyme EII (Varghese et al. 1994), illustrating an approximately 40-Å-long substrate-binding cleft (left image) with nucleophilic E232 and the most likely catalytic acid E93 (cpk sticks), and the docked G4G3G4G4G4G3G4G$_{red}$ (cpk sticks) oligosaccharide (right image). Dispositions of carboxylates indicate the cleavage point of the (1;3,1;4)-β-oligoglucoside (arrows).

The X-ray crystal structures showed that both the (1,3)-β-glucanase and the (1,3;1,4)-β-glucanase adopt $(\alpha/\beta)_8$ barrel conformations, with deep substrate-binding clefts about 40 Å long extending across the surfaces of the enzymes (Varghese et al. 1994; Fig. 3B). This is consistent with the enzymes' endo-acting action patterns, whereby internal linkages of the polysaccharides can be hydrolyzed essentially at random, depending on the position of substrate binding across the cleft. The catalytic acid residues are E93 and E94 and the catalytic nucleophiles are E231 and E232 for the (1,3)-β-glucanase and the (1,3;1,4)-β-glucanase, respectively (Henrissat et al. 1995; Jenkins et al. 1995; Fig. 3B).

Superposition of the polypeptide backbones of the barley (1,3)-β-glucanase isoenzyme GII and the (1,3;1,4)-β-glucanase isoenzyme EII showed a very high level of correspondence in the 3D dispositions of the Cα backbones of the 2 enzymes. The root-mean-square-deviation value in Cα positions was 0.65 Å over 278 amino acid residues (out of a total of 306 residues) (Varghese et al. 1994). This indicated a close evolutionary relationship between the 2 enzymes. (1,3;1,4)-β-Glucanases most likely evolved from the (1,3)-β-glucanases, because (1,3)-β-glucanases are much more widely distributed across the plant kingdom and mediate in multiple plant functions. Consistent with the more recent evolution of the (1,3;1,4)-β-glucanases, there are only 2 known (1,3;1,4)-β-glucanase genes in the barley genome (Woodward and Fincher 1982; Mascher et al. 2017), whereas the (1,3)-β-glucanase gene families across plants are relatively large, with up to 70 members in some plant genomes (Drula et al. 2022). It is noteworthy that the (1,3;1,4)-β-glucan synthases of the CslF subfamily evolved from the CesA and CslD (1,4)-β-glucan synthases, whereas the (1,3;1,4)-β-glucan endohydrolases evolved from the (1,3)-β-glucan endohydrolases.

Hydrolysis of (1,3;1,4)-β-glucans: The remarkable enzymic mechanism of a barley β-glucan exohydrolase and trajectories of the reactants

Polysaccharide exohydrolases and enzymes classified as glycosidases, usually in concert with endoglucanases, are important in depolymerization processes in which a

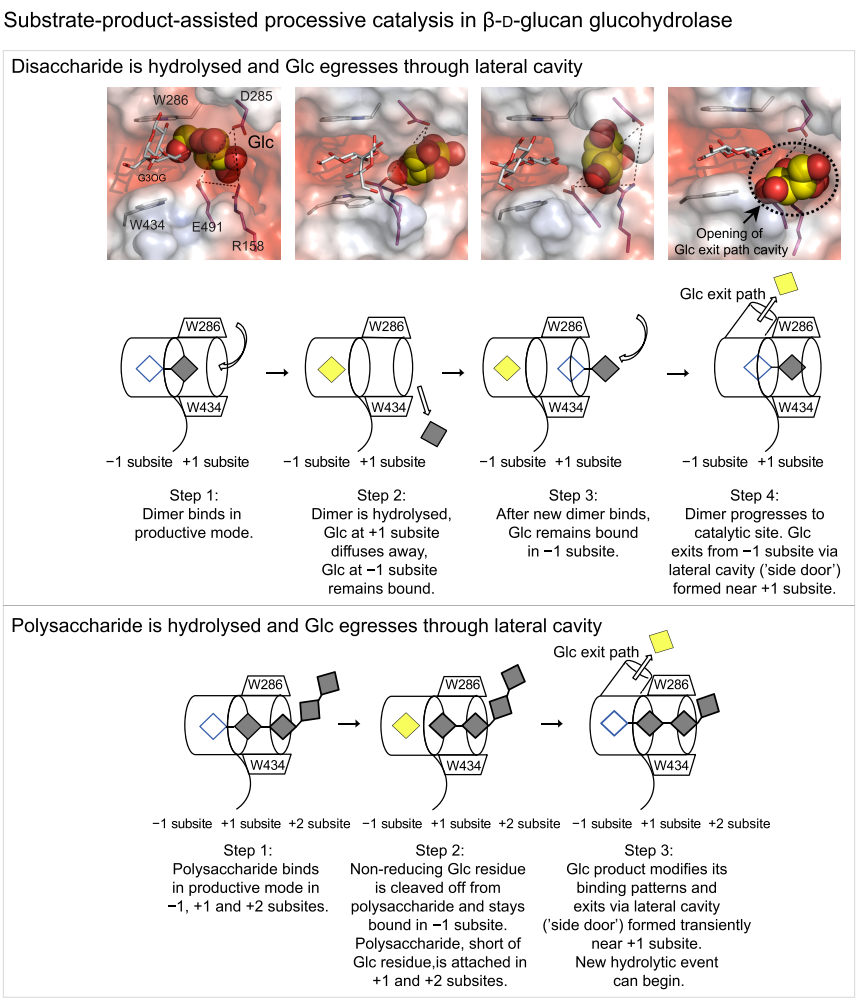

Figure 4. Substrate-product-assisted processivity of the barley β-D-glucan glucohydrolase, isoenzyme *Exo*1. **A)** Displacement pathway of the Glc product (Streltsov et al. 2019). Top panels: Four steps along the Glc displacement route (cpk yellow spheres) released from laminaribiose (cpk sticks). Surfaces of β-D-glucan glucohydrolase are coloured by electrostatic potentials (white, neutral; blue; +5 kT·e^{-1}; red, −5 kT·e^{-1}, respectively). Steps 1 to 4: Glc is in the −1 subsite; step 2: movements of R158, D285, and E491 (cpk sticks; distances in dashes) allow Glc to traverse into the transient lateral cavity; step 3: Glc in the cavity is partly exposed to the bulk solvent; step 4: Glc is fully exposed to the bulk solvent and leaves through the solvent-exposed aperture of the transient lateral cavity (black dotted ellipsoid with arrow). Middle panels: Mechanism of Glc exit path from laminaribiose. After the disaccharide (empty blue and filled grey squares) enters through the W286 and W434 clamp (curved arrow), it binds in the −1 and +1 subsites (step 1) and is hydrolyzed with an aglycon diffusing away (step 2). Glc (yellow square) remains non-covalently trapped through multiple hydrogen bonds. After a new substrate binds (large arrow) and advances to the catalytic site (step 3), Glc modifies its binding patterns

(continued)

polysaccharide is completely hydrolyzed to its constituent monosaccharides. One group of β-glucan exohydrolases purified from young barley seedlings has been shown to exhibit a broad substrate specificity that enables the hydrolytic removal of single Glc molecules from the nonreducing termini of a range of polysaccharides and oligosaccharides, including (1,3)-β-glucans, (1,6)-β-glucans, (1,3;1,4)-β-glucans, (1,3;1,6)-β-glucans, and (1,2)-, (1,3)-, (1,4)-, and (1,6)-β-glucosyl oligosaccharides and aryl glucosides (Hrmova et al. 1996; Hrmova and Fincher 1998, 2007). The functions of the enzymes in young barley seedlings are likely to include the turnover of (1,3;1,4)-β-glucans during normal growth and development and during light/dark growth periods and the hydrolysis of fungal cell wall (1,3)-β-glucans, (1,6)-β-glucans, and (1,3;1,6)-β-glucans following pathogenic attack (Roulin et al. 1997, 2002).

The barley β-glucan exohydrolases are classified in the large GH3 family of glycoside hydrolases, which catalyze exohydrolysis of a range of substrates, with retention of anomeric configuration (Fig. 4A; Hrmova et al. 1996; Drula et al. 2022). There are up to 12 β-glucan exohydrolase genes in the barley genome (M. Hrmova, unpublished data). Comparative specific activities of the barley Exo1 isoenzyme for barley (1,3;1,4)-β-glucan, 4-nitrophenyl β-glucoside, cellopentaose, and laminarin are 1.0 : 1.3 : 2.3 : 16.3 units/mg, respectively (Hrmova et al. 1996).

A high-resolution 3D structure of the barley β-glucan exohydrolase isoenzyme *Exo*1 was determined to 2.2-Å resolution by X-ray crystallography by Varghese et al. (1999) (PDB accession 1ex1). The enzyme is a globular protein of 605 amino acid residues that has an $(\alpha/\beta)_8$ barrel domain and a 6-stranded $(\alpha/\beta)_6$ sandwich domain; 602 amino acid residues are represented in the 3D structure. The 6-stranded $(\alpha/\beta)_6$ sandwich domain consists of a β-sheet of 5 parallel β-strands and 1 antiparallel β-strand, with 3 α-helices on either side of the sheet (Varghese et al. 1999). The active site forms an enclosed, dead-end pocket about 13 Å deep at the interface of the 2 domains. The pocket includes 2 glucosyl-binding subsites (−1 and +1) (Hrmova et al. 2002), together with the E491 catalytic acid/base and the D285 catalytic nucleophile (Varghese et al. 1999; Hrmova et al. 2001). In an another study it was established that the barley β-glucan exohydrolase proceeds through the ^{4}E (envelope) transition state (Hrmova et al. 2004, 2005) (PDB accession 1lq2). To determine the conformational landscape and the dynamic behavior of the saccharide moiety-binding modes, molecular dynamics (MD) simulation analyses of positionally isomeric disaccharides (PDB accessions 3wlp, 6jg1, 6jg2, 6jg7) showed that HvExo1 hydrolyzing laminaribiose exhibits a 2-fold hydrolytic itinerary, which starts either from a distorted $^4H_3/^4E/^4H_5$ region or from an undistorted $^4C_1$ β-D-glucopyranosyl ring, which would evolve toward a transition state with a $^4H_3/^4E$ conformation in both cases (Luang et al. 2022).

The broad specificity of the enzyme and hence its potential role in diverse functions during plant growth and development is explained by the presence of 2 Trp residues (W286 and W434) at the entrance to the active site pocket. The entrance has the appearance of a coin slot that is bound by W286 from domain 1 on 1 side and by W434 from domain 2 on the other side. Two glucosyl residues of the nonreducing end of the polysaccharide occupy the active site pocket, while the remainder of the polysaccharide substrate protrudes from the active site in a disordered state. The nonreducing terminal glucosyl residue is at the bottom of the pocket and is tightly bound through extensive hydrogen bonding in substrate-binding subsite −1 (Hrmova et al. 2002). The penultimate glucosyl residue is clamped in subsite +1 between the 2 Trp residues at the mouth of the pocket. The relatively broad area of the heterocyclic indole moieties of the Trp residues and the fact that they constrain the penultimate glucosyl less tightly than the terminal glucosyl residue is bound means that the third and subsequent residues away from the mouth of the coin slot are free to project in various directions from the enzyme's surface (Hrmova et al. 2002). It is this relative freedom of orientation permitted by the W286/W434 aromatic clamp at subsite +1 that allows different types of glycosidic linkages to be bound in the active site of the enzyme (Luang et al. 2022).

Based on the shape of the substrate-binding pocket and the bound glucose that is eventually released from the substrate at the bottom of the pocket, one would expect that the polysaccharide substrate would need to dissociate from the enzyme's surface after each hydrolytic event to allow the released Glc to diffuse out of the active site pocket. The polysaccharide chain would re-associate with the

Figure 4. (Continued)
and exits (side arrow) via the lateral cavity (drawn as a cylinder) formed near the catalytic site (step 4). Bottom panels: Mechanism of Glc displacement pathway from a polysaccharide. After nonreducing (blue square) and penultimate (filled square) residues bind in a productive mode at the −1 and +1 subsites (step 1), the nonreducing Glc (yellow square) is cleaved off, with the remainder of the substrate attached (step 2). Glc (yellow square) modifies its binding patterns and is released (large arrow) via the lateral cavity (cylinder, step 3). The next hydrolytic cycle proceeds with the same polysaccharide, where the substrate is short of 1 Glc residue, continues sliding into the active site after uninterrupted binding. **B)** The Glc egress trajectory (Luang et al. 2022), illustrated on the top of the enzyme's surface, is colored by an electrostatic potential with bound Glc (cpk yellow sticks) and laminaribiose (cpk sticks). The trajectory (yellow spheres) represents frames that correspond to consecutive stages of Glc egress with conforming coordinates for Glc in each frame. Multi-scale molecular modelling of nanoscale reactant movements was conducted using docking and MD simulations (Jones et al. 1997), GaudiMM (Rodríguez-Guerra Pedregal et al. 2017), PELE (Borrelli et al. 2005), and GPathFinder (Sánchez-Aparicio et al. 2019).

Table 1. 3D structures of plant enzymes, deposited in the protein data bank (PDB; April 28, 2023), involved in synthesis, re-modelling, and hydrolysis of plant cell wall polysaccharides

Enzyme/source	Description/EC number	PDB accession	Reference
Glycoside hydrolases			
(1,3)-β-Glucanase isoenzyme GII/*Hordeum vulgare* L.	(1,3)-β-D-Glucan endohydrolase/EC 3.2.1.39	1ghs	Varghese et al. (1994)
(1,3;1,4)-β-Glucanase isoenzyme EII/*Hordeum vulgare* L.	(1,3;1,4)-β-D-Glucan endohydrolase/EC 3.2.1.73	1ghr 1aq0	Varghese et al. (1994) Müller et al. (1998)
β-Glucan exohydrolase isoenzyme Exo1/*Hordeum vulgare* L.	β-D-Glucan exohydrolase/EC 3.2.1.-	1ex1, 1ieq, 1iev, 1iew, 1iex, 1jv8, 1lq2, 1 × 38, 1 × 39, 3wlh, 2wli, 3wlj, 3wlk, 3wlm, 3wln, 3wlo, 3wlp, 3wlq, 3wlr, 3wls, 3wlt, 6jg1, 6jg2, 6jg6, 6jg7, 6jga, 6jgb, 6jgc, 6jgd, 6jge, 6jgg, 6jgk, 6jgl, 6jgn, 6jgo, 6jgp, 6jgq, 6jgr, 6jgs, 6jgt, 6k6v, 6kuf, 6l1j, 6lbb, 6lbv, 6lc5, 6md6, 6mi1—in complex with substrate analogues and mimics	Hrmova et al. (1998) Varghese et al. (1999) Hrmova et al. (2001) Hrmova et al. (2002) Hrmova et al. (2004) Hrmova et al. (2005) Luang et al. (2022)
PttXET16A/*Populus tremulus x tremuloides* L.	Xyloglucan xyloglucosyl transferase/EC 2.4.1.207	1un1 1 μmz—in complex with xyloglucan hexa-saccharide	Johansson et al. (2004)
NXG1/NXG1/NXG1-delta-YNII/NXG2/*Tropaeolum majus* L.	Endo-xyloglucanase/EC 3.2.1.151	2uwa 2vh9—in complex with xyloglucan nona-saccharide 2uwb 2uwc	Baumann et al. (2007)
Endo-1,4-β-xylanase/*Scadoxus multiflorus*	(1,4)-β-D-Xylan endohydrolase/EC 3.2.1.8	3m7s—in complex with cellobiose	Kumar et al. (2010)
VvEG16/*Vitis vinifera* L.	Xyloglucan-specific endo-β-D-1,4-glucanase EC 3.2.1.151	5dze—in complex with glucose and tetra-saccharide 5dzf—in complex with glucose, tetra-saccharide and octa-saccharide 5dzg—in complex with xyloglucan hepta- and tetradeca-saccharide 5sv8—in complex with xyloglucan hexa-saccharide	McGregor et al. (2017)
Polygalacturonase/*Arabidopsis thaliana* (L.) Heynh.	Endo-polygalacturonase/EC 3.2.1.15	7b7a 7b8b	Safran et al. (2022) (unpublished)
Carbohydrate esterases			
Pectin methylesterase/*Daucus carota* L.	Pectin methyl esterase EC 3.1.1.11	1gq8	Johansson et al. (2002)
Pectin methylesterase/*Lycopersicon esculentum* L.	Pectin methyl esterase EC 3.1.1.11	1xg2—in complex with a pectinesterase inhibitor	Di Matteo et al. (2005)
Glycosyl transferases			
AtFUT1/*Arabidopsis thaliana* (L.) Heynh.	Xyloglucan fucosyltransferase/EC 2.4.1.69	5kop—in complex with Cl^- 5kor—in complex with Cl^-, GDP and xyloglucan nona-saccharide	Rocha et al. (2016a, 2016b)
AtXXT1/*Arabidopsis thaliana* (L.) Heynh.	Xyloglucan xylosyltransferase/EC 2.4.2.39	6bsu—in complex with Mn^{2+}	Culbertson et al. (2018)
Cellulose synthase isoform 8/*Populus tremulus x tremuloides* L.	Cellulose synthase/EC 2.4.1.12	6wlb—in complex with cello-pentaose 8g27—in complex with UDP, Mg^{2+} ions and cellopentaose 8g2j—in complex with UDP-Glc, Mg^{2+} and cello-pentaose	Purushotham et al. (2020) Verma et al. (2023)
Cellulose synthase isoform 7/*Gossypium hirsutum* L.	Cellulose synthase/EC 2.4.1.12	7d5k—in complex with cellobiose	Zhang et al. (2021b)
Cellulose synthase A3 catalytic domain/*Arabidopsis thaliana* (L.) Heynh.	Cellulose synthase/EC 2.4.1.12	7ck3 7ck2—in complex with Mn^{2+} and UDP-Glc 7ck1—in complex with Mn^{2+}	Qiao et al. (2021)
CslF6/*Hordeum vulgare* L.	(1,3;1,4)-β-Glucan synthase/EC 2.4.1.-	8dqk	Purushotham et al. (2022)
GalS1/*Populus trichocarpa* L.	(1,4)-β-Galactan synthase/EC 2.4.1.-	8d3t 8d3z—in complex with Mn^{2+}	Prabhakar et al. (2023)

enzyme before the second hydrolytic event. However, the observation that a Glc glucose molecule remained trapped in subsite −1 at the bottom of the pocket until an incoming substrate bound to the enzyme raised the question as to why this product of the reaction had not diffused away (Hrmova et al. 2002).

In addressing this knowledge gap on the importance of substrate association pathways onto the enzyme and product dissociation pathways away from the enzyme, Streltsov et al. (2019) discovered a previously unknown and remarkable enzymic mechanism for this polysaccharide exohydrolase, which they coined "substrate-product assisted

processive catalysis," using high-resolution X-ray crystallography of thio-glucoside enzyme complexes (PDB accessions 3wlo, 3wlr, 6md6, 6mi1) and MD simulations. Following hydrolysis of the nonreducing terminal glycosidic linkage, the polysaccharide remains bound to the enzyme, and the released Glc, which occupies substrate-binding subsite −1, is ejected from the active site through a "side door." The "side door" opens into a lateral tunnel that acts as a conduit for egress of the Glc product when the polysaccharide substrate binds to the enzyme. Opening occurs through rotations and backbone movements of several amino acid residues within the active site pocket, including D285, E491, and R158 (Streltsov et al. 2019; Fig. 4, A and B). As the released Glc exits, the substrate, which remains bound by the W286/W434 aromatic clamp at original substrate-binding subsite +1, is pulled into the active site pocket through dispersive forces and the hydrolytic events are repeated. This processive catalysis mechanism applies only to the hydrolysis of (1,3)-β-glucans. Hydrolysis of the other substrates, including the (1,3;1,4)-β-glucans, involves dissociation and re-association of the substrate following each hydrolytic event (Streltsov et al. 2019; Luang et al. 2022). Removing the need for the polysaccharide substrate to diffuse away from and subsequently re-bind to the enzyme after each hydrolytic event results in the much higher catalytic rate and specific activity for this enzyme with (1,3)-β-glucan substrates, as noted above. This study suggested that processive catalysis might be prevalent amongst other exohydrolases of the GH3 family of enzymes.

Luang et al. (2022) used high-resolution X-ray crystallography (PDB accessions 3wli, 3wlo, 6jg1, and 6jg2) and multiscale molecular modeling of wild-type and a mutant barley β-glucan exohydrolase isoenzyme *Exo*1 to define the precise molecular mechanism and the trajectories of the reactants and products in nanoscale time and space. This demonstrated the coordination of substrate binding, hydrolysis, and Glc product egress through the transient "side door" (Fig. 4B) and further showed that processivity was sensitive to specific alterations of the W286/W434 tryptophan clamp. Additional phylogenomic analyses of GH3 hydrolases revealed the evolutionary advantage of the Trp clamp, which confers broad specificity, high catalytic efficiency, and processivity in selected groups of GH3 exohydrolase (Luang et al. 2022; Hrmova and Schwerdt 2023).

3D structures of other enzymes involved in plant cell wall metabolism

As noted above, defining the 3D structures of integral membrane enzymes is technically challenging. In addition to the solved structures of the GT2 subfamily CesA8 and CslF6 enzymes, further insights into the structure and function of integral membrane proteins have recently been expanded through the structures of non-plant enzymes, namely an oomycete and a fungal chitin synthase (Chen et al. 2022; Ren et al. 2022) and a yeast (1,3)-β-glucan synthase (Hu et al. 2023). These belong to the GT2 and GT48 enzyme families, respectively.

Returning to higher plant enzymes that are involved in wall synthesis, the following structures have been solved: a solubilized (transmembrane anchor removed) Arabidopsis family GT37 xyloglucan fucosyltransferase (*At*FUT1; Protein Data Bank-PDB-accession 5kop) (Rocha et al. 2016a, 2016b; Urbanowicz et al. 2017), an Arabidopsis family GT34 xyloglucan xylosyltransferase (*At*XXT1; PDB accession 6bsu) (Culbertson et al. 2018), and a *Populus trichocarpa* family GT92 (1,4)-β-galactan synthase (GalS1; PDB accession 8d3t) (Prabhakar et al. 2023). These structures have provided valuable insights into the mechanisms of xyloglucan and pectic polysaccharide synthesis. However, the FUT1, XXT1, and GalS1 enzymes are nonprocessive and catalyze the addition of monosaccharide moieties (or single glycosyl residues of side chains) to nascent xyloglucans and pectic polysaccharides. Because (1,3;1,4)-β-glucans are linear, unbranched, unsubstituted polysaccharides they do not require these classes of glycosyl transferases for their synthesis. The FUT1, XXT1, and GalS1 enzymes are peripheral membrane proteins that retain their 3D structures and hence their activity when displaced from membranes with mild detergent treatment. These enzymes can also be expressed in heterologous systems in an active, soluble form if the membrane anchor coding region is removed.

Similarly, the enzymes that catalyze the depolymerization and remodeling of wall polysaccharides are generally soluble proteins that are amenable to crystallization and hence 3D structural analysis. In Table 1, we have listed the current PDB database-registered 3D structures of enzymes involved in plant cell wall synthesis, remodeling, and hydrolysis. It shows that 3D structures have been determined for fewer than 20 enzymes involved in these processes in plants. One can argue that this is a relatively modest number considering the total number of enzymes involved (Zhang et al. 2021a; Yokoyama 2020; McFarlane 2023) and the functional, evolutionary, and mechanistic insights that can be revealed through these structures.

Future opportunities

Cell walls of barley and oat grains contain relatively high levels of (1,3;1,4)-β-glucans. These polysaccharides are not digested in the human small intestine and therefore represent important components of dietary fiber, which reduces the risk of serious diseases, including type II diabetes (Jacobs and Gallaher 2004; Dikeman and Fahey 2006), colorectal cancer (Bingham et al. 2003), and cardiovascular disease (Jacobs and Gallaher 2004; Collins et al. 2010). The beneficial effects of these polysaccharides may, in part at least, be attributable to alterations in the bacterial microbiome of the large intestine induced by (1,3;1,4)-β-glucans in the diet (Gorham et al. 2017). Human gut metagenomes confirm the importance of specific gut bacteria in the metabolism of (1,3;1,4)-β-glucans in human diets

OUTSTANDING QUESTIONS BOX

- What are the molecular mechanisms of the synthetic enzymes that allow the percentages and sequences of the DP3, DP4 and higher oligocellulosic groups to be manipulated to change the physicochemical properties of the (1,3;1,4)-β-glucans?
- What is the evolutionary origin and how was the selection pressure applied to give rise to the substrate-product–assisted processivity in GH3 hydrolases?
- Are other polysaccharide non-GH3 exohydrolase enzymes capable of processive action mechanisms?
- How can AlphaFold protein structure and AlphaFill predictions be used to identify the substrate specificities of enzymes involved in the synthesis and depolymerization of other cell wall polysaccharides?

(Martens et al. 2011; Tamura et al. 2017; Déjean et al. 2020; Singh et al. 2023).

Burton et al. (2011) showed that overexpression of the *CslF6* gene in transgenic barley increased levels of grain (1,3;1,4)-β-glucan by up to 80% (w/w) or more in grain and leaves of the transgenic lines and that overexpression of the *CslF* genes led to statistically validated ($P < 0.05$) changes of up to 25% in the DP3:DP4 ratios of grain (1,3;1,4)-β-glucan of transgenic lines, depending on the *CslF* gene used. As described above, DP3:DP4 ratios are related to (1,3;1,4)-β-glucan solubility and although the mechanisms that control DP3:DP4 ratios have not yet been defined, the results of Burton et al. (2011) indicate that within barley there is a genetic basis for the control of the ratio and hence for the solubility of the polysaccharide. The cryo-EM structure of the CslF6 enzyme and the definition of the mechanism for (1,3)-linkage insertion (Purushotham et al. 2022) is an important first step toward understanding how the variations in DP3:DP4 ratios are regulated. Generating a higher resolution 3D structure for the CslF6 enzyme in complex with reactants or their homologues is considered an important next step in defining how the fine structure of the polysaccharide is controlled. This, in turn, would allow the design of high (1,3;1,4)-β-glucan grain for the production of health foods and beverages with high levels of soluble dietary fiber. This approach could be equally applied for designer production of synthases of other polysaccharides that have health benefits or are used in industrial processes, including thickeners in foods and liquids, malting and brewing, bioethanol production, and related bioconversion processes for renewable energy production. The same applications will also benefit from 3D structural analyses and attendant advances in our understanding of (1,3;1,4)-β-glucanases, XETs and other hydrolytic enzymes that mediate the metabolism of cell wall polysaccharides.

In a more general sense, the development and public release of the AlphaFold artificial intelligence program by Deep Mind and an associated AlphaFill algorithm have provided extraordinary opportunities for the international plant cell wall community (Callaway 2020; Jumper et al. 2021; Hekkelman et al. 2022). The ability to rapidly and accurately predict a protein's 3D shape from its amino acid sequence, coupled with substrate docking and MD programs, will enable the functions of genes and enzymes known or suspected to be involved in wall synthesis, degradation, or modification to be identified and subsequently tested. Nevertheless, X-ray crystallography and cryo-EM will remain as highly useful experimental approaches for the solving and confirmation of 3D structures (Terwilliger et al. 2022, 2023). In this review, we have shown how the 3D structure of the barley CslF6 (1,3;1,4)-β-glucan synthase, determined by cryo-EM and refined using the AlphaFold-predicted model, can lead not only to a description of the enzyme's mechanism of action but can also reveal potential routes for the improvement or adaption of the enzyme for a variety of novel functional objectives. In another hypothetical example, the 3D structure of an undefined member of say the CslE subfamily of GT2 enzymes could be predicted by AlphaFold and a range of potential sugar nucleotide substrates could be modeled into its putative active site using AlphaFill and other algorithms, thereby providing a testable hypothesis on the function of the enzyme. Given the very large number of enzymes and proteins that participate in plant cell wall metabolism, fascinating opportunities are presented by these new experimental and theoretical structural biology approaches.

Acknowledgments

We acknowledge the dedicated work of our postgraduate students, postdoctoral scientists, and other colleagues over many years. We dedicate this review to Professor Bruce Stone, who maintained a life-long fascination with the biosynthetic mechanism of (1,3;1,4)-β-glucan biosynthesis and hydrolysis.

Author contributions

M.H. and J.Z. contributed 3D images, V.B. was responsible for product analyses, G.F. prepared the first draft of the manuscript. All authors contributed to the finalization of the manuscript.

Funding

This work was supported by grants from the NIH (grants SIG S10-RR025067 and U24-GM116790), the Center for Ligno cellulose Structure and Formation, an Energy Frontier Research Center funded by the U.S. Department of Energy, Office of

Science, Basic Energy Sciences (award DESC0001090), and the Australian Research Council's Centre of Excellence in Plant Cell Walls (grant no. CE1101007). V.B. was supported by an ARC Discovery Project grant (grant no. DP180103974). J.Z. is a Howard Hughes Medical Institute Investigator. M.H. is supported by the University of Adelaide and the Waite Research Institute.

Conflict of interest statement. The authors could identify no conflicts of interest.

Data availability

The author responsible for distribution of materials integral to the findings presented in this article in accordance with the policy described in the Instructions for Authors (https://academic.oup.com/plphys/pages/general-instructions) is Geoff Fincher (geoff.fincher@adelaide.edu.au).

Note added in proof

After this manuscript was accepted for publication, we became aware of a paper describing the synthesis of (1,3;1,4)-β-D-glucan in bacteria (**Lee J, Hollingsworth RI** Oligosaccharide β-glucans with unusual linkages from *Sarcina ventriculi*. Carbohydr Res 1997:**304**:133–141), which was recently confirmed by Chang et al. (**Chang SC, Kao MR, Saldivar RK, Díaz-Moreno SM, Xing X, Furlanetto V, Yayo J, Divne C, Vilaplana F, Abbott DW, Hsieh YSY** The Gram-positive bacterium *Romboutsia ilealis* harbors a polysaccharide synthase that can produce (1,3;1,4)-β-D-glucans. Nat Commun 2023:**14**:4526, doi: 10.1038/s41467-023-40214-z). Thus, enzymes capable of synthesizing these polysaccharides have evolved in bacteria, fungi, algae and both lower and higher plants.

References

Akdemir KH, Seven M, Derman ÜC, Harvey AJ. *In silico* analysis of XTH gene family from barley (*Hordeum vulgare* L.) and their comparative expression analysis during germination. Turkish J Bot. 2022:**46**(2):Article 1. https://doi.org/10.55730/1300-008X.2674

Anderson MA, Stone BA. A new substrate for investigating the specificity of β-glucan hydrolases. FEBS Lett. 1975:**52**(2):202–207. https://doi.org/10.1016/0014-5793(75)80806-4

Bartesaghi A, Merk A, Banerjee S, Matthies D, Wu X, Milne JL, Subramaniam S. 2.2 Å resolution cryo-EM structure of β-galactosidase in complex with a cell-permeant inhibitor. Science. 2015:**348**(6239):1147–1151. https://doi.org/10.1126/science.aab1576

Baumann MJ, Eklöf JM, Michel G, Kallas AM, Teeri TT, Czjzek M, Brumer H 3rd. Structural evidence for the evolution of xyloglucanase activity from xyloglucan endo-transglycosylases: biological implications for cell wall metabolism. Plant Cell. 2007:**19**(6):1947–1963. https://doi.org/10.1105/tpc.107.051391

Behar H, Graham SW, Brumer H. Comprehensive cross-genome survey and phylogeny of glycoside hydrolase family 16 members reveals the evolutionary origin of EG 16 and XTH proteins in plant lineages. Plant J. 2018:**95**(6):1114–1128. https://doi.org/10.1111/tpj.14004

Bernal JD. Dr Rosalind E. Franklin. Nature. 1958:**182**(4629):154. https://doi.org/10.1038/182154a0

Bernal J, Yoo CM, Mutwil M, Jensen JK, Hou G, Blaukopf C, Sorensen I, Blancaflor EB, Scheller HV, Willats WGT. Functional analysis of the cellulose synthase-like genes *CSLD1*, *CSLD2*, and *CSLD4* in tip-growing Arabidopsis cells. Plant Physiol. 2008:**148**(3):1238–1253. https://doi.org/10.1104/pp.108.121939

Bingham SA, Day NE, Luben R, Ferrari P, Slimani N, Norat T, Clavel-Chapelon F, Kesse E, Nieters A, Boeing H, et al. Dietary fibre in food and protection against colorectal cancer in the European prospective investigation into cancer and nutrition (EPIC): an observational study. Lancet. 2003:**361**(9368):1496–1501. https://doi.org/10.1016/S0140-6736(03)13174-1

Borrelli KW, Vitalis A, Alcantara R, Guallar V. PELE: protein energy landscape exploration. a novel Monte Carlo-based technique. J Chem Theory Comput. 2005:**1**(6):1304–1311. https://doi.org/10.1021/ct0501811

Buckeridge MS, Vergara CE, Carpita NC. Insight into multi-site mechanisms of glycosyl transfer in (1→4)-β-d-glycans provided by the cereal mixed-linkage (1→3), (1→4)–β–d-glucan synthase. Phytochemistry. 2001:**57**(7):1045–1053. https://doi.org/10.1016/S0031-9422(01)00110-8

Buliga GS, Brandt DA, Fincher GB. The sequence statistics and solution conformation of a barley (1→3,1→4)-β- d-glucan. Carbohydr Res. 1986:**157**:139–156. https://doi.org/10.1016/0008-6215(86)85065-0

Bulone V, Schwerdt JG, Fincher GB. Adoption of evolving technologies to define cell wall biology in the grasses: a brief but unfinished history. In press in: **Geitmann A**, editor. *Plant cell walls – research milestones and conceptual insights*. Milton Park, Oxfordshire, UK: CRC Press, Taylor & Francis Group; 2023.

Burton RA, Collins HM, Kibble NAJ, Smith JA, Shirley NJ, Jobling SA, Henderson M, Singh RR, Pettolino F, Wilson SM, et al. Over-expression of specific *HvCslF* cellulose synthase-like genes in transgenic barley increases the levels of cell wall (1,3; 1,4)-β- d-glucans and alters their fine structure. Plant Biotechnol J. 2011:**9**(2):117–135. https://doi.org/10.1111/j.1467-7652.2010.00532.x

Burton RA, Fincher GB. (1,3; 1,4)-β-d-glucans in cell walls of the Poaceae, lower plants and fungi: a tale of two linkages. Mol Plant. 2009:**2**(5):873–882. https://doi.org/10.1093/mp/ssp063

Burton RA, Gidley MJ, Fincher GB. Heterogeneity in the chemistry, structure and function of plant cell walls. Nat Chem Biol. 2010:**6**(10):724–732. https://doi.org/10.1038/nchembio.439

Burton RA, Jobling SA, Harvey AJ, Shirley NJ, Mather DE, Bacic A, Fincher GB. The genetics and transcriptional profiles of the cellulose synthase-like *HvCslF* gene family in barley (*Hordeum vulgare* L.). Plant Physiol. 2008:**146**(4):1821–1833. https://doi.org/10.1104/pp.107.114694

Burton RA, Wilson SM, Hrmova M, Harvey AJ, Shirley NJ, Medhurst A, Stone BA, Newbigin EJ, Bacic A, Fincher GB. Cellulose synthase-like *CslF* genes mediate the synthesis of cell wall (1,3; 1,4)-β-D-glucans. Science. 2006:**311**(5769):1940–1942. https://doi.org/10.1126/science.1122975

Callaway E. 'It will change everything' DeepMind's AI makes gigantic leap in solving protein structures. Nature. 2020:**588**(7837):203–205. https://doi.org/10.1038/d41586-020-03348-4

Carpita NC, McCann MC. The maize mixed-linkage (1→3), (1→4)-β-D-glucan polysaccharide is synthesized at the Golgi membrane. Plant Phys. 2010:**153**(3):1362–1371. https://doi.org/10.1104/pp.110.156158

Cate JH, Gooding AR, Podell E, Zhou K, Golden BL, Kundrot CE, Cech TR, Doudna JA. Crystal structure of a group 1 ribozyme domain: principles of RNA packing. Science. 1996:**273**(5282):1678–1685. https://doi.org/10.1126/science.273.5282.1678

Chen W, Cao P, Liu Y, Yu A, Wang D, Chen L, Sundarraj R, Yuchi Z, Gong Y, Merzendorfer H, et al. Structural basis for directional chitin biosynthesis. Nature. 2022:**610**(7931):402–408. https://doi.org/10.1038/s41586-022-05244-5

Chen L, Fincher GB, Høj PB. Evolution of polysaccharide hydrolase substrate specificity. Catalytic amino acids are conserved in barley 1,3-1,4- and 1,3-beta-glucanases. J Biol Chem. 1993:**268**(18):13318–13326. https://doi.org/10.1016/S0021-9258(19)38654-5

Collins HM, Burton RA, Topping DL, Liao M-L, Bacic A, Fincher GB. Variability in the fine structures of non-cellulosic cell wall polysaccharides from cereal grains: potential importance in human health and nutrition. Cereal Chem. 2010:**87**(4):272–282. https://doi.org/10.1094/CCHEM-87-4-0272

Corey RB, Pauling LC. Fundamental dimensions of polypeptide chains. Proc R Soc Lond B Biol Sci. 1953:**141**(902):10–20. https://doi.org/10.1098/rspb.1953.0011

Culbertson AT, Ehrlich JJ, Choe JY, Honzatko RB, Zabotina OA. Structure of xyloglucan xylosyltransferase 1 reveals simple steric rules that define biological patterns of xyloglucan polymers. Proc Natl Acad Sci USA. 2018:**115**(23):6064–6069. https://doi.org/10.1073/pnas.1801105115

Déjean G, Tamura K, Cabrera A, Jain N, Pudlo NA, Pereira G, Viborg AH, Van Petegem F, Martens EC, Brumer H. Synergy between cell surface glycosidases and glycan-binding proteins dictates the utilization of specific beta (1, 3)-glucans by human gut *Bacteroides*. MBio. 2020:**11**(2):e00095-20. https://doi.org/10.1128/mBio.00095-20

Dhugga KS. Biosynthesis of non-cellulosic polysaccharides of plant cell walls. Phytochemistry. 2012:**74**:8–19. https://doi.org/10.1016/j.phytochem.2011.10.003

Dikeman CL, Fahey GC. Viscosity as related to dietary fiber: a review. Crit Rev Food Sci. 2006:**46**(8):649–663. https://doi.org/10.1080/10408390500511862

Di Matteo A, Giovane A, Raiola A, Camardella L, Bonivento D, De Lorenzo G, Cervone F, Bellincampi D, Tsernoglou D. Structural basis for the interaction between pectin methylesterase and a specific inhibitor protein. Plant Cell. 2005:**17**(3):849–858. https://doi.org/10.1105/tpc.104.028886

Dimitroff G, Little A, Lahnstein J, Schwerdt JG, Shirley NJ, Burton RA, Fincher GB. (1,3; 1,4)-β-glucan biosynthesis by the CSLF6 enzyme: position and flexibility of catalytic residues influence product fine structure. Biochemistry. 2016:**55**(13):2054–2061. https://doi.org/10.1021/acs.biochem.5b01384

Doblin MS, De Melis L, Newbigin E, Bacic A, Read SM. Pollen tubes of *Nicotiana alata* express two genes from different beta-glucan synthase families. Plant Physiol. 2001:**125**(4):2040–2052. https://doi.org/10.1104/pp.125.4.2040

Drula E, Garron M-L, Dogan S, Lombard V, Henrisatt B, Terrapon N. The carbohydrate-active enzyme database: functions and literature. Nucleic Acids Res. 2022:**50**(D1):D571–D577. https://doi.org/10.1093/nar/gkab1045

Eklöf JM, Brumer H. The *XTH* gene family: an update on enzyme structure, function, and phylogeny in xyloglucan re-modelling. Plant Physiol. 2010:**153**(2):456–466. https://doi.org/10.1104/pp.110.156844

Fincher GB, Stone BA. Chemistry of non-starch polysaccharides from cereal grains. In: **Wrigley C Corke H, Walker CE**, editors. Encyclopedia of grain science, Vol. 1. Cambridge, MA: Elsevier Academic Press; 2004. p. 206–223.

Garcia-Gimenez G, Barakate A, Smith P, Stephens J, Khor S, Doblin M, Hao P, Bacic A, Fincher GB, Burton RA, et al. Targeted mutation of barley (1,3; 1,4)-β-glucan synthases reveals complex relationships between the storage and cell wall polysaccharide content. Plant J. 2020:**104**(4):1009–1022. https://doi.org/10.1111/tpj.14977

Gidley MJ, Nishinari K. Physico-chemistry of (1,3)-β-glucans. In: **Stone BA, Bacic A, Fincher GB**, editors. Chemistry, biochemistry, and biology of (1-3)-β-glucans and related polysaccharides. Philadelphia (PA), USA: Elsevier Inc.; 2009. p. 47–118.

Gorham JB, Kang S, Williams BA, Grant LJ, McSweeney CS, Gidley MJ, Mikkelsen D. Addition of arabinoxylan and mixed linkage glucans in porcine diets affects the large intestinal bacterial populations. European J Nutr. 2017:**56**(6):2193–2206. https://doi.org/10.1007/s00394-016-1263-4

Guillon F, Larré C, Petipas F, Berger A, Moussawi J, Rogniaux H, Santoni A, Saulnier L, Jamme F, Miquel M, et al. A comprehensive overview of grain development in *Brachypodium distachyon* variety Bd21. J Exp Bot. 2012:**63**(2):739–755. https://doi.org/10.1093/jxb/err298

Harris PJ, Fincher GB. Distribution, fine structure and function of (1,3; 1,4)-β-glucans in the grasses and other taxa. In: **Stone BA, Bacic T, Fincher GB**, editors. Chemistry, biochemistry, and biology of (1,3)-β-glucans and related polysaccharides. Philadelphia (PA), USA: Elsevier Inc.; 2009. p. 621–654.

Hekkelman ML, de Vries I, Joosten RP, Perrakis A. Alphafill: enriching AlphaFold models with ligands and cofactors. Nat Methods. 2022:**20**(2):205–213. https://doi.org/10.1038/s41592-022-01685-y

Henrissat B, Callebaut I, Fabrega S, Lehn P, Mornon JP, Davies G. Conserved catalytic machinery and the prediction of a common fold for several families of glycosyl hydrolases. Proc Natl Acad Sci USA. 1995:**92**(15):7090–7094. https://doi.org/10.1073/pnas.92.15.7090

Hrmova M, De Gori R, Smith BJ, Fairweather JK, Driguez H, Varghese JN, Fincher GB. Structural basis for broad substrate specificity in higher plant β-d-glucan glucohydrolases. Plant Cell. 2002:**14**(5):1033–1052. https://doi.org/10.1105/tpc.010442

Hrmova M, De Gori R, Smith BJ, Vasella A, Varghese JN, Fincher GB. Three-dimensional structure of the barley β-d-glucan glucohydrolase in complex with a transition state mimic. J Biol Chem. 2004:**279**(6):4970–4980. https://doi.org/10.1074/jbc.M307188200

Hrmova M, Farkas V, Harvey AJ, Lahnstein J, Wischmann B, Kaewthai N, Ezcurra I, Teeri TT, Fincher GB. Substrate specificity and catalytic mechanism of a xyloglucan xyloglucosyl transferase HvXET6 from barley (*Hordeum vulgare* L). FEBS Journal. 2009:**276**(2):437–456. https://doi.org/10.1111/j.1742-4658.2008.06791.x

Hrmova M, Farkas V, Lahnstein J, Fincher GB. A barley xyloglucan xyloglucosyl transferase covalently links xyloglucan, cellulosic substrates and (1,3; 1,4)-β-d-glucans. J Biol Chem. 2007:**282**(17):12951–12962. https://doi.org/10.1074/jbc.M611487200

Hrmova M, Fincher GB. Barley β-d-glucan exohydrolases. Substrate specificity and kinetic properties. Carbohydr Res. 1998:**305**(2):209–221. https://doi.org/10.1016/S0008-6215(97)00257-7

Hrmova M, Fincher GB. Dissecting the catalytic mechanism of a plant β-d-glucan glucohydrolase through inhibitors, substrate analogues and structural biology. Carbohydr Res. 2007:**342**(12-13):1613–1623. https://doi.org/10.1016/j.carres.2007.05.013

Hrmova M, Harvey AJ, Wang J, Shirley NJ, Jones GP, Stone BA, Høj PB, Fincher GB. Barley β-d-glucan exohydrolases with β-glucosidase activity. Purification, characterization and determination of primary structure from a cDNA clone. J Biol Chem. 1996:**271**(9):5277–5286. https://doi.org/10.1074/jbc.271.9.5277

Hrmova M, Schwerdt JG. Molecular mechanisms of processive glycoside hydrolases underline catalytic pragmatism. Biochem Soc Trans. 2023:**51**(3):1387–1403. https://doi.org/10.1042/BST20230136

Hrmova M, Streltsov VA, Smith BJ, Vasella A, Varghese JN, Fincher GB. Structural rationale for low nanomolar binding of transition state mimics to a family GH3 β-D-glucan glucohydrolase from barley. Biochemistry. 2005:**44**(50):16529–16539. https://doi.org/10.1021/bi0514818

Hrmova M, Varghese JN, De Gori R, Smith BJ, Driguez H, Fincher GB. Catalytic mechanisms and reaction intermediates along the hydrolytic pathway of plant β-d-glucan glucohydrolase. Structure. 2001:**9**(11):1015–1016. https://doi.org/10.1016/S0969-2126(01)00673-6

Hrmova M, Varghese JN, Høj PB, Fincher GB. Crystallization and preliminary X-ray analysis of β-glucan exohydrolase isoenzyme ExoI from barley (*Hordeum vulgare*). Acta Crystallogr D Biol Crystallogr. 1998:**54**(4):687–689. https://doi.org/10.1107/S0907444997018866

Hu X, Yang P, Chai C, Liu J, Sun H, Wu Y, Zhang M, Zhang M, Liu X, Yu H. Structural and mechanistic insights into fungal β-1,3-glucan synthase FKS1. Nature. 2023:**616**(7955):190–198. https://doi.org/10.1038/s41586-023-05856-5

Jacobs DR, Gallaher DD. Whole grain intake and cardiovascular disease: a review. Curr Atheroscler Rep. 2004:**6**(6):415–423. https://doi.org/10.1007/s11883-004-0081-y

Jarvis MC. Structure of native cellulose microfibrils, the starting point for nanocellulose manufacture. Philos Trans A Math Phys Eng Sci. 2018:**376**(2112):20170045. https://doi.org/10.1098/rsta.2017.0045

Jenkins J, Lo Leggio L, Harris G, Pickersgill R. β-Glucosidase, β-galactosidase, family A cellulases, family F xylanases and two barley glycanases form a superfamily of enzymes with 8-fold β/α architecture and with two conserved glutamates near the carboxy-terminal ends of β-strands four and seven. FEBS Lett. 1995:**362**(3):281–285. https://doi.org/10.1016/0014-5793(95)00252-5

Jobling SA. Membrane pore architecture of the CslF6 protein controls (1-3,1-4)-β-glucan structure. Sci Adv. 2015:**1**(5):e1500069. https://doi.org/10.1126/sciadv.1500069

Johansson P, Brumer H 3rd, Baumann MJ, Kallas AM, Henriksson H, Denman SE, Teeri TT, Jones TA. Crystal structures of a poplar xyloglucan endotransglycosylase reveal details of transglycosylation acceptor binding. Plant Cell. 2004:**16**(4):874–886. https://doi.org/10.1105/tpc.020065

Johansson K, El-Ahmad M, Friemann R, Jörnvall H, Markovic O, Eklund H. Crystal structure of plant pectin methylesterase. FEBS Lett. 2002:**514**(2-3):243–249. https://doi.org/10.1016/S0014-5793(02)02372-4

Jones G, Willett P, Glen RC, Leach AR, Taylor R. Development and validation of a genetic algorithm for flexible docking. J Mol Biol. 1997:**267**(3):727–748. https://doi.org/10.1006/jmbi.1996.0897

Jumper J, Evans R, Pritzel A, Green T, Figurnov M, Ronneberger O, Tunyasuvunakool K, Bates R, Žídek A, Potapenko A, et al. Highly accurate protein structure prediction with AlphaFold. Nature. 2021:**596**(7873):583–589. https://doi.org/10.1038/s41586-021-03819-2

Kim SJ, Zemelis S, Keegstra K, Brandizzi F. The cytoplasmic localization of the catalytic site of CSLF6 supports a channeling model for the biosynthesis of mixed-linkage glucan. Plant J. 2015:**81**(4):537–547. https://doi.org/10.1111/tpj.12748

Kühlbrandt W. The resolution revolution. Science. 2014:**343**(6178):1443–1444. https://doi.org/10.1126/science.1251652

Kumar S, Singh N, Sinha M, Dube D, Singh SB, Bhushan A, Kaur P, Srinivasan A, Sharma S, Singh TP. Crystal structure determination and inhibition studies of a novel xylanase and alpha-amylase inhibitor protein (XAIP) from *Scadoxus multiflorus*. FEBS J. 2010:**277**(13):2868–2882. https://doi.org/10.1111/j.1742-4658.2010.07703.x

Lairson LL, Henrissat B, Davies GJ, Withers SG. Glycosyltransferases: structures, functions, and mechanisms. Annu Rev Biochem. 2008:**77**(1):521–555. https://doi.org/10.1146/annurev.biochem.76.061005.092322

Lazaridou A, Biliaderis CG. Molecular aspects of cereal β-glucan functionality: physical properties, technological applications and physiological effects. J Cereal Sci. 2007:**46**(2):101–118. https://doi.org/10.1016/j.jcs.2007.05.003

Little A, Schwerdt JG, Shirley NJ, Khor SF, Neumann K, O'Donovan LA, Lahnstein J, Collins HM, Henderson M, Fincher GB, et al. Revised phylogeny of the *cellulose synthase* gene superfamily: insights into cell wall evolution. Plant Physiol. 2018:**177**(3):1124–1141. https://doi.org/10.1104/pp.17.01718

Luang S, Fernández-Luengo X, Nin-Hill A, Streltsov VA, Schwerdt JG, Alonso-Gil S, Ketudat Cairns JR, Pradeau S, Fort S, Maréchal J-D, et al. The evolutionary advantage of an aromatic clamp in plant family 3 glycoside exo-hydrolases. Nat Commun. 2022:**13**(1):5577. https://doi.org/10.1038/s41467-022-33180-5

Maloney FP, Kuklewicz J, Corey RA, Bi YC, Ho RY, Mateusiak L, Pardon E, Steyaert J, Stansfeld PJ, Zimmer J. Structure, substrate recognition and initiation of hyaluronan synthase. Nature. 2022:**604**(7904):195–201. https://doi.org/10.1038/s41586-022-04534-2

Martens EC, Lowe EC, Chiang H, Pudlo NA, Wu M, McNulty NP, Abbott DW, Henrissat B, Gilbert HJ, Bolam DN, et al. Recognition and degradation of plant cell wall polysaccharides by two human gut symbionts. PLoS Biol. 2011:**9**(12):e1001221. https://doi.org/10.1371/journal.pbio.1001221

Mascher M, Gundlach H, Himmelbach A, Beier S, Twardziok S, Wicker T, Radchuk V, Dockter C, Hedley P, Russell J, et al. A chromosome conformation capture ordered sequence of the barley genome. Nature. 2017:**544**(7651):427–433. https://doi.org/10.1038/nature22043

McFarlane HE. Open questions in plant cell wall synthesis. J Exp Bot . 2023:**74**:3425–3448. https://doi.org/10.1093/jxb/erad110

McGregor N, Yin V, Tung CC, Van Petegem F, Brumer H. Crystallographic insight into the evolutionary origins of xyloglucan endotransglycosylases and endohydrolases. Plant J. 2017:**89**(4):651–670. https://doi.org/10.1111/tpj.13421

Morgan JL, McNamara JT, Fischer M, Rich J, Chen HM, Withers SG, Zimmer J. Observing cellulose biosynthesis and membrane translocation *in crystallo*. Nature. 2016:**531**(7594):329–334. https://doi.org/10.1038/nature16966

Morgan J, Strumillo J, Zimmer J. Crystallographic snapshot of cellulose synthesis and membrane translocation. Nature. 2013:**493**(7431):181–186. https://doi.org/10.1038/nature11744

Müller JJ, Thomsen KK, Heinemann U. Crystal structure of barley 1,3-1,4-beta-glucanase at 2.0-A resolution and comparison with Bacillus 1,3-1,4-beta-glucanase. J Biol Chem. 1998:**273**(6):3438–3446. https://doi.org/10.1074/jbc.273.6.3438

Namchuk MN, Withers SG. Mechanism of Agrobacterium α-glucosidase: kinetic analysis of the role of non-covalent enzyme substrate interactions. Biochemistry. 1995:**34**(49):16194–16202. https://doi.org/10.1021/bi00049a035

Nemeth C, Freeman J, Jones HD, Sparks C, Pellny TK, Wilkinson MD, Dunwell J, Andersson AAM, Åman P, Guillon F, et al. Down-regulation of the *CSLF6* gene results in decreased (1,3;1,4)-*β*-D-glucan in endosperm of wheat. Plant Physiol. 2010:**152**(3):1209–1218. https://doi.org/10.1104/pp.109.151712

Okekeogbu IO, Pattathil S, González Fernández-Niño SM, Aryal UK, Penning BW, Lao J, Heazlewood JL, Hahn MG, McCann MC, Carpita NC. Glycome and proteome components of Golgi membranes are common between two angiosperms with distinct cell-wall structures. Plant Cell. 2019:**31**(5):1094–1112. https://doi.org/10.1105/tpc.18.00755

Orlean P, Funai D. Priming and elongation of chitin chains: implications for chitin synthase mechanism. Cell Surf. 2019:**1**(5):100017. https://doi.org/10.1016/j.tcsw.2018.100017

Park S, Szumlanski AL, Gu F, Guo F, Nielsen E. A role for CSLD3 during cell-wall synthesis in apical plasma membranes of tip-growing root-hair cells. Nature Cell Biol. 2011:**13**(8):973–980. https://doi.org/10.1038/ncb2294

Pauly M, Gille S, Liu L, Mansoori N, de Souza A, Schultink A, Xiong G. Hemicellulose biosynthesis. Planta. 2013:**238**(4):627–642. https://doi.org/10.1007/s00425-013-1921-1

Prabhakar PK, Pereira JH, Taujale R, Shao W, Bharadwaj VS, Chapla D, Yang JY, Bomble YJ, Moremen KW, Kannan N, et al. Structural and biochemical insight into a modular β-1,4-galactan synthase in plants. Nat Plants. 2023:**9**(3):486–500. https://doi.org/10.1038/s41477-023-01358-4

Purushotham P, Cho SH, Diaz-Moreno SM, Kumar M, Nixon BT, Bulone V, Zimmer J. A single heterologously expressed plant cellulose synthase isoform is sufficient for cellulose microfibril formation *in vitro*. Proc Natl Acad Sci USA. 2016:**113**(40):11360–11365. https://doi.org/10.1073/pnas.1606210113

Purushotham P, Ho R, Yu L, Fincher GB, Bulone V, Zimmer J. Mechanism of mixed linkage glucan biosynthesis by barley cellulose synthase-like CslF6 (1,3; 1,4)-β-glucan synthase. Sci Adv. 2022:**8**(45):eadd1596. https://doi.org/10.1126/sciadv.add1596

Purushotham P, Ho R, Zimmer J. Architecture of a catalytically active homotrimeric plant cellulose synthase complex. Science. 2020:**369**(6507):1089–1094. https://doi.org/10.1126/science.abb2978

Qiao Z, Lampugnani ER, Yan XF, Khan GA, Saw WG, Hannah P, Qian F, Calabria J, Miao Y, Grüber G, et al. Structure of *Arabidopsis* CESA3 catalytic domain with its substrate UDP-glucose provides insight into the mechanism of cellulose synthesis. Proc Natl Acad Sci USA. 2021:**118**(11):e2024015118. https://doi.org/10.1073/pnas.2024015118

Ren Z, Chhetri A, Guan Z, Suo Y, Yokoyama K, Lee SY. Structural basis for inhibition and regulation of a chitin synthase from *Candida albicans*. Nat Struct Molec Biol. 2022:**29**(7):653–664. https://doi.org/10.1038/s41594-022-00791-x

Richmond TA, Somerville CR. The cellulose synthase superfamily. Plant Physiol. 2000:**124**(2):495–498. https://doi.org/10.1104/pp.124.2.495

Rocha J, Cicéron F, de Sanctis D, Lelimousin M, Chazalet V, Lerouxel O, Breton C. Structure of *Arabidopsis thaliana* FUT1 reveals a variant of the GT-B class fold and provides insight into xyloglucan fucosylation. Plant Cell. 2016b:**28**(10):2352–2364. https://doi.org/10.1105/tpc.16.00519

Rocha J, Cicéron F, Lerouxel O, Breton C, de Sanctis D. The galactoside 2-α-L-fucosyltransferase FUT1 from *Arabidopsis thaliana*: crystallization and experimental MAD phasing. Acta Crystallogr F Struct Biol Commun. 2016a:**72**(7):564–568. https://doi.org/10.1107/S2053230X16009584

Rodríguez-Guerra Pedregal J, Sciortino G, Guasp J, Municoy M, Maréchal J-D. GaudiMM: a modular multi-objective platform for molecular modeling. J Comput Chem. 2017:**38**(24):2118–2126. https://doi.org/10.1002/jcc.24847

Roulin S, Buchala AJ, Fincher GB. Induction of (1→3,1→4)-β-glucan hydrolases in leaves of dark-incubated barley seedlings. Planta. 2002:**215**(1):51–59. https://doi.org/10.1007/s00425-001-0721-1

Roulin S, Xu P, Brown AHD, Fincher GB. Expression of specific (1→3)-β-glucanase genes in leaves of near-isogenic resistant and susceptible barley lines infected with the scald fungus (*Rhynchosporium secalis*). Physiol Molec Plant Pathol. 1997:**50**(4):245–261. https://doi.org/10.1006/pmpp.1997.0084

Safran J, Tabi W, Ung V, Lemaire A, Habrylo O, Bouckaert J, Rouffle M, Voxeur A, Pongrac P, Bassard S, Molinié R. Differences in the structure of plant polygalacturonases specify enzymes' dynamics and processivities to fine-tune cell wall pectins. bioRxiv. 2022 Jun 23:2022-06.

Sánchez-Aparicio JE, Sciortino G, Herrmannsdoerfer DV, Chueca PO, Pedregal JR, Maréchal J-D. GPathfinder: identification of ligand binding pathways by a multi-objective genetic algorithm. Int J Mol Sci. 2019:**20**(13):3155. https://doi.org/10.3390/ijms20133155

Scavuzzo-Duggan TR, Chaves AM, Singh A, Sethaphong L, Slabaugh E, Yingling YG, Haigler CH, Roberts AW. Cellulose synthase 'class specific regions' are intrinsically disordered and functionally undifferentiated. J Integr Plant Biol. 2018:**606**(6):481–497. https://doi.org/10.1111/jipb.12637

Schwerdt JG, MacKenzie K, Wright F, Oemhe D, Wagner JM, Harvey AJ, Shirley NJ, Burton RA, Wright F, MacKenzie K, et al. Evolutionary dynamics of the cellulose synthase gene superfamily in grasses. Plant Physiol. 2015:**168**(3):968–983. https://doi.org/10.1104/pp.15.00140

Sethaphong L, Haigler CH, Kubicki JD, Zimmer J, Bonetta D, DeBolt S, Yingling YG. Tertiary model of a plant cellulose synthase. Proc Natl Acad Sci USA. 2013:**110**(18):7512–7517. https://doi.org/10.1073/pnas.1301027110

Seven M, Derman ÜC, Harvey AJ. Enzymatic characterization of ancestral/group-IV clade xyloglucan endotransglycosylase/hydrolase enzymes reveals broad substrate specificities. Plant J. 2021:**106**(6):1660–1673. https://doi.org/10.1111/tpj.15262

Singh RP, Niharika J, Thakur R, Wagstaff BA, Kumar G, Kurata R, Patel D, Levy CW, Miyazaki T, Field RA. Utilization of dietary mixed-linkage β-glucans by the firmicute Blautia producta. J Biol Chem. 2023:**299**(6):104806. https://doi.org/10.1016/j.jbc.2023.104806

Sinnott ML. Catalytic mechanism of enzymic glycosyl transfer. Chem Rev. 1990:**90**(7):1171–1202. https://doi.org/10.1021/cr00105a006

Smith MM, Stone BA. β-Glucan synthesis by cell-free extracts from *Lolium multiflorum* endosperm. Biochim Biophys Acta Gen Subj. 1973:**313**(1):72–94. https://doi.org/10.1016/0304-4165(73)90189-X

Staudte RG, Woodward JR, Fincher GB, Stone BA. Water-soluble (1→3), (1→4)-β-d-glucans from barley (*Hordeum vulgare*) endosperm. III. Distribution of cellotriosyl and cellotetraosyl residues. Carbohydr Polym. 1983:**3**(4):299–312. https://doi.org/10.1016/0144-8617(83)90027-9

Stratilová B, Šesták S, Mravec J, Garajová S, Vadinová K, Kučerová D, Kozmon S, Schwerdt JG, Shirley N, Hrmova M, et al. Another building block in the plant cell wall: barley xyloglucan xyloglucosyl transferases link covalently xyloglucan and anionic oligosaccharides derived from pectin. Plant J. 2020:**104**(3):752–767. https://doi.org/10.1111/tpj.14964

Streltsov VA, Luang S, Peisley A, Varghese JN, Ketudat Cairns JR, Fort S, Hijnen M, Tvaroška I, Ardá A, Hrmova M, et al. Discovery of processive catalysis by an exo-hydrolase with a pocket-shaped active site. Nat Commun. 2019:**10**(1):2222. https://doi.org/10.1038/s41467-019-09691-z

Taketa S, Yuo T, Tonooka T, Tsumuraya Y, Inagaki Y, Haruyama N, Larroque O, Jobling SA. Functional characterization of barley betaglucanless mutants demonstrates a unique role for *CslF6* in (1,3;1,4)-β-D-glucan biosynthesis. J Exp Bot. 2011:**63**(1):381–392. https://doi.org/10.1093/jxb/err285

Tamura K, Hemsworth GR, Déjean G, Rogers TE, Pudlo NA, Urs K, Jain N, Davies GJ, Martens EC, Brumer H. Molecular mechanism by which prominent human gut Bacteroidetes utilize mixed-linkage beta-glucans, major health-promoting cereal polysaccharides. Cell Rep. 2017:**21**(2):417–430. https://doi.org/10.1016/j.celrep.2017.09.049

Terwilliger TC, Afonine PV, Liebschner D, Croll TI, McCoy AJ, Oeffner RD, Williams CJ, Poon BK, Richardson JS, Read RJ, et al. Accelerating crystal structure determination with iterative AlphaFold prediction. Acta Crystallogr D Struct Biol. 2023:**79**(Pt 3):234–244. https://doi.org/10.1107/S205979832300102X

Terwilliger TC, Leibschner DL, Croll T, Williams CJ, McCoy AJ, Poon BK, Afonine P, Oeffner RD, Richardson JS, Read RJ, et al. Alphafold predictions: great hypotheses but no match for experiment. bioRxiv 517405. https://doi.org/10.1101/2022.11.21.517405, 22 November 2022, preprint: not peer reviewed.

Trafford K, Haleux P, Henderson M, Parker M, Shirley NJ, Tucker MR, Fincher GB, Burton RA. Grain development in *Brachypodium* and other grasses: interactions between cell expansion, starch deposition and cell wall synthesis. J Exp Bot. 2013:**64**(16):5033–5047. https://doi.org/10.1093/jxb/ert292

Urbanowicz BR, Bharadwaj VS, Alahuhta M, Pena MJ, Lunin VV, Bomble YJ, Wang S, Yang JY, Tuomivaara ST, Himmel ME, et al. Structural, mutagenic and *in silico* studies of xyloglucan fucosylation in *Arabidopsis thaliana* suggest a water-mediated mechanism. Plant J. 2017:**91**(6):931–949. https://doi.org/10.1111/tpj.13628

van de Meene A, McAloney L, Wilson SM, Zhou J, Zeng W, McMillan P, Bacic A, Doblin MS. Interactions between cellulose and (1,3;1,4)-β-glucans and arabinoxylans in the regenerating wall of suspension culture cells of the ryegrass *Lolium multiflorum*. Cells. 2021:**11**(1):127. https://doi.org/10.3390/cells10010127

Varghese JN, Garrett TPJ, Colman PM, Chen L, Høj PB, Fincher GB. The three-dimensional structures of two plant β-glucan endohydrolases with distinct substrate specificities. Proc Natl Acad Sci USA. 1994:**91**(7):2785–2789. https://doi.org/10.1073/pnas.91.7.2785

Varghese JN, Hrmova M, Fincher GB. Three-dimensional structure of a barley β-d-glucan exohydrolase; a family 3 hydrolase. Structure. 1999:**7**(2):179–190. https://doi.org/10.1016/S0969-2126(99)80024-0

Vega-Sánchez ME, Verhertbruggen Y, Christensen U, Chen X, Sharma V, Varanasi P, Jobling SA, Talbot M, White RG, Joo M, et al. Loss of cellulose synthase-like F6 function affects mixed-linkage glucan deposition, cell wall mechanical properties, and defense responses in vegetative tissues of rice. Plant Physiol. 2012:**159**(1):56–69. https://doi.org/10.1104/pp.112.195495

Verma P, Kwansa AL, Ho R, Yingling YG, Zimmer J. Insights into substrate coordination and glycosyl transfer of poplar cellulose synthase-8. bioRxiv 527505. https://doi.org/10.1101/2023.02.07.527505, 7 February 2023, preprint: not peer reviewed.

Viborg AH, Terrapon N, Lombard V, Michel G, Czjzek M, Henrissat B, Brumer H. A subfamily roadmap of the evolutionarily diverse glycoside hydrolase family 16 (GH16). J Biol Chem. 2019:**294**(44): 15973–15986. https://doi.org/10.1074/jbc.RA119.010619

Wang JY, Pausch P, Doudna JA. Structural biology of CRISPR–Cas immunity and genome editing enzymes. Nat Rev Microbiol. 2022:**20**(11):641–656. https://doi.org/10.1038/s41579-022-00739-4

Watson JD, Crick FH. Molecular structure of nucleic acids: a structure for deoxyribose nucleic acid. Nature. 1953:**171**(4356):737–738. https://doi.org/10.1038/171737a0

Weigel PH, DeAngelis PL. Hyaluronan synthases: a decade-plus of novel glycosyltransferases. J Biol Chem. 2007:**282**(51):36777–36781. https://doi.org/10.1074/jbc.R700036200

Wightman R, Turner SR. The roles of the cytoskeleton during cellulose deposition at the secondary cell wall. Plant J. 2008:**54**(5):794–805. https://doi.org/10.1111/j.1365-313X.2008.03444.x

Wilson SM, Ho YY, Lampugnani ER, van de Meene AML, Bain MP, Bacic A, Doblin MS. Determining the subcellular location of synthesis and assembly of the cell wall polysaccharide (1,3; 1,4)-β-D-glucan in grasses. Plant Cell. 2015:**27**(3):754–771. https://doi.org/10.1105/tpc.114.135970

Woodward JR, Fincher GB. Purification and chemical properties of two (1,3:1,4)-β-glucan endohydrolases from germinating barley. Eur J Biochem. 1982:**121**(3):663–669. https://doi.org/10.1111/j.1432-1033.1982.tb05837.x

Woodward JR, Fincher GB, Stone BA. Water-soluble (1→3), (1→4)-β-d-glucans from barley (*Hordeum vulgare*) endosperm. II. Fine structure. Carbohydr Polym. 1983:**3**(3):207–225. https://doi.org/10.1016/0144-8617(83)90019-X

Yang J, Bak G, Burgin T, Barnes WJ, Mayes HB, Pena MJ, Urbanowicz BR, Nielsen E. Cellulose synthase-like D (CSLD) 3 protein is a beta-1,4-glucan synthase. Plant Cell. 2020:**32**(5):1749–1767. https://doi.org/10.1105/tpc.19.00637

Yin Y, Johns MA, Cao H, Rupani M. A survey of plant and algal genomes and transcriptomes reveals new insights into the evolution and function of the cellulose synthase superfamily. BMC Genom. 2014:**15**(1):260. https://doi.org/10.1186/1471-2164-15-260

Yip KM, Fischer N, Paknia E, Chari A, Stark H. Atomic-resolution protein structure determination by cryo-EM. Nature. 2020:**587**(7832): 157–161. https://doi.org/10.1038/s41586-020-2833-4

Yokoyama R. A genomic perspective on the evolutionary diversity of the plant cell wall. Plants. 2020:**9**(9):1195. https://doi.org/10.3390/plants9091195

Zhang B, Gao Y, Zhang L, Zhou Y. The plant cell wall: biosynthesis, construction, and functions. J Integr Plant Biol. 2021a:**63**(1): 251–272. https://doi.org/10.1111/jipb.13055

Zhang X, Xue Y, Guan Z, Zhou C, Nie Y, Men S, Wang Q, Shen C, Zhang D, Jin S, et al. Structural insights into homotrimeric assembly of cellulose synthase CesA7 from *Gossypium hirsutum*. Plant Biotechnol J. 2021b:**19**(8):1579–1587. https://doi.org/10.1111/pbi.13571